Chaotic fluctuations in Greenland ~~outlet glaciers~~ ice streams limit predictability of ~~a future~~ ice sheet collapse

Kolja Kypke [1,2], Marisa Montoya [3,4], Alexander Robinson [5], Jorge Alvarez-Solas [3,4], Jan Swierczek-Jereczek [3,4], and Peter Ditlevsen [1]

[1]Department of Mathematics and Statistics, University of Guelph, Guelph, Canada
[2]Physics of Ice, Climate and Earth, Niels Bohr Institute, University of Copenhagen, Copenhagen, Denmark
[3]Department of Earth Physics and Astrophysics, Complutense University of Madrid, Madrid, Spain
[4]Geosciences Institute, CSIC–UCM, Madrid, Spain
[5]Alfred Wegener Institute, Helmholtz Centre for Polar and Marine Research, Potsdam, Germany

Correspondence: Kolja Kypke (kkypke@uoguelph.ca)

Abstract. The future evolution of the Greenland ice sheet (GrIS) depends on the intensity and the speed of climate change. By applying different rates of temperature change in a state-of-the-art comprehensive ice-sheet model coupled to a regional energy-moisture balance atmospheric model, oscillations in the total ice-sheet volume are found under warming magnitudes between 1.0 and 1.3 K above present-day temperatures. These are located in the northwestern drainage basin of the GrIS and are due to two ice streams which alternate between fast and slow basal velocities, manifesting in a build-up/surge variability. These ice streams interact due to their spatial proximity, resulting in irregular periodicity. The ice streams appear in a region where tipping of the entire GrIS begins, leading the oscillations to affect the tipping behaviour. These oscillations directly impact the time it takes before the ice sheet collapses at a given external forcing magnitude by hundreds of thousands of years for an ensemble of rates of forcing and initial conditions. These long tipping times are proposed to be due to chaotic transients. Our results suggest that ice-stream oscillations are a potential source of internal chaotic variability in ice sheets that affect tipping behaviour, thereby complicating prospects of anticipating such a tipping.

1 Introduction

The Greenland ice sheet (GrIS) is one of the principal tipping elements in Earth's climate system (Armstrong McKay et al., 2022), meaning it could experience a massive and potentially irreversible change when an external forcing parameter, specifically the global mean temperature, increases beyond a critical threshold known as a 'tipping point' (Robinson et al., 2012). This phenomenon is also termed 'bifurcation-induced tipping' (b-tipping). This tipping involves the large-scale loss of ice mass (or 'collapse' of the ice sheet) through melting and has a straightforward impact on the rest of the Earth by raising the global sea level ~~(Gregory et al., 2004; Rignot et al., 2011)~~(Gregory et al., 2004; Rignot et al., 2011; Wunderling et al., 2021).

Tipping of the GrIS can occur due to the presence of two strong positive feedbacks: First, a decrease in ice-sheet thickness means that the temperature of the ice surface increases, promoting further melting~~,~~. This is known as the melt-elevation feedback. The second is the decrease of the surface albedo as a result of the retreat of the ice sheet increasing the amount of

solar energy absorbed, known as the ice-albedo feedback. In steady state, where the ice sheet is in mass balance, the dynamics must, however, be dominated by negative feedbacks: As atmospheric temperatures increase, so does the precipitation and the surface mass balance, leading to a thickening of the ice sheet. Furthermore, the melt-elevation feedback is reduced by the effect of glacial isostatic adjustment: when ice thins, the resulting bedrock uplift partially compensates the reduced surface elevation and thus the surface melt. This effect is, however, mainly relevant on long time scales (Wake et al., 2016; Zeitz et al., 2022). The atmospheric temperature is considered the critical parameter. As it increases, the negative feedbacks weaken and at the bifurcation point, ~~the negative feedback~~ they no longer control the state and the positive feedbacks will force it into the alternative state.

The feedbacks that determine the stability of the GrIS are influenced strongly by the surface air temperature of Greenland, which is increasing at a rapid pace (Intergovernmental Panel On Climate Change (IPCC), 2023). While the critical temperature for tipping of the GrIS has been assessed in different studies ~~(?Höning et al., 2023; Robinson et al., 2012; Zeitz et al., 2022)~~ (Gutiérrez-González et al., 2026; Höning et al., 2023; Robinson et al., 2012; Zeitz et al., 2022), the effect of the rate of change of the forcing on the tipping behaviour has ~~not yet been investigated . The feedbacks that determine the stability of the GrIS are influenced strongly by the surface air temperature of Greenland, which is increasing at a rapid pace (Intergovernmental Panel On Climate Ch~~ only been investigated for the Antarctic ice sheet (Feldmann et al., 2025; Swierczek-Jereczek et al., 2025). In non-autonomous systems with multiple dynamic time scales, high rates of forcing compared to the time scale for restoring to the equilibrium state could lead to a tipping of the system at a forcing less than the bifurcation point, a phenomenon known as 'rate-induced tipping' (r-tipping) (Ashwin et al., 2012; Feudel, 2023).

The bulk of the GrIS evolves over time according to slow shear flow, but areas of fast flowing ice, such as topographically confined outlet glaciers or large ice streams, represent a source of variability with a faster dynamic timescale. Ice streams~~in particular are relevant, as they~~ , which are characterized by sliding of ice at the base due to ~~a~~ lubrication over a hard base or deformation of a till that is saturated with water, are particularly relevant. A fast warming rate can lead to an easier saturation of the base ~~because it~~ with water that cannot be compensated by ~~the drainage rate~~drainage from under the ice sheet, activating ice streams and increasing mass loss. The discharge of ice through ice streams contributes a large amount to the total ice-sheet mass loss despite their relatively small spatial extent (The IMBIE Team, 2020; Van Den Broeke et al., 2009). Furthermore, ice streams have accelerated due to increased atmospheric and oceanic ~~forcing~~forcings, contributing up to 50% of the GrIS mass loss in the last decades ~~(Holland et al., 2008; Howat et al., 2008; Khan et al., 2014; Krabill et al., 2004; Larocca et al., 2023; Luthcke et al., 2006; Rig~~ (Box et al., 2022; Howat et al., 2008; Khan et al., 2014, 2022; Larocca et al., 2023; Luthcke et al., 2006; Rignot and Kanagaratnam, 2006; .

Rate-induced tipping of a component of the Earth system has been investigated previously in comprehensive models of the Atlantic Meridional Overturning Circulation (AMOC) (Lohmann and Ditlevsen, 2021) and the west Antarctic ice sheet (Swierczek-Jereczek et al., 2025). The rate of forcing is also important when considering the ~~ability to prevent~~ possibility of preventing a transition after overshooting a tipping point by imposing a subsequent cooling (Bochow et al., 2023). In this study, we use a state-of-the-art ice-sheet model coupled to a regional atmospheric energy-moisture balance model to investigate the GrIS response under different magnitudes and rates of warming in order to determine whether r-tipping of the GrIS is possible.

2 Methods

2.1 Model description

The model used in this study is the three-dimensional thermomechanical ice-sheet model Yelmo ~~(Robinson et al., 2020)~~ (Robinson et al., 2020, 2022) coupled with the regional energy-moisture balance climate model REMBO (Robinson et al., 2010) at the ice-sheet surface. This model setup is similar to that of Robinson et al. (2012) but with a ~~newer~~ different ice-sheet model, and has also been used in the study of Gutiérrez-González et al. (2026). The model domain covers the entirety of Greenland at a horizontal resolution of 16 km. ~~The surface mass balance (SMB) is determined by the temperature and precipitation calculated by REMBO. The SMB can be separated into a positive contribution from the precipitation and a negative contribution resulting from surface melt. The latter is calculated using an insolation-temperature melt method (ITM), whereby insolation and albedo are explicitly taken into account. The isostatic adjustment of the bedrock under the ice sheet uses the elastic lithosphere-relaxing asthenosphere (ELRA) model (Meur and Huybrechts, 1996) with a relaxation timescale of 3000 years.~~

~~To compute the icedynamics, Yelmo uses the depth-integrated viscosity approximation (Goldberg, 2011; Robinson et al., 2022)~~

The description of the ice-sheet model is not repeated here. Instead we focus on the description of the processes that occur at the base of the ice, which rely on several parameterizations and are important for the results of this article, are included in this section. The basal frictional stress ~~$\boldsymbol{\tau}_b = (\tau_{b,x}, \tau_{b,y})$~~ $\boldsymbol{\tau}_b$ is modelled using a regularized Coulomb friction law (Schoof, 2005; Joughin et al., 2019),

$$\boldsymbol{\tau}_b = -c_b \left(\frac{|\mathbf{u}_b|}{|\mathbf{u}_b| + u_0} \right)^q \frac{\mathbf{u}_b}{|\mathbf{u}_b|}, \tag{1}$$

where ~~$\mathbf{u_b} = (u_b, v_b)$ is the~~ $\mathbf{u_b}$ is the two-dimensional basal velocity vector, ~~$u_0 = 100$ m a^{-1} and $q = 0.2$ are empirical parameters derived from laboratory experiments (Zoet and Iverson, 2020), and c_b is a field defining the bed-friction coefficient~~. The threshold speed ~~u_0~~ $u_0 = 100$ m a^{-1} allows the basal stress to saturate at large velocities, where it becomes independent of basal velocity (Blasco et al., 2024; Zoet and Iverson, 2020). ~~The~~ Its value, along with the empirical parameter $q = 0.2$, are derived from laboratory experiments (Zoet and Iverson, 2020). The bed friction coefficient c_b is a field that depends linearly on the effective pressure N at the base of the ice,

$$c_b = \lambda N. \tag{2}$$

The factor λ represents the till strength of the bedrock and depends on the elevation above or below sea level. This factor leads to increased sliding velocity by reducing basal friction at lower elevations, owing to the till in these areas being composed primarily of sediments that are softer and more easily deformable. A similar elevation-dependent till strength is also seen in Albrecht et al. (2020) and Martin et al. (2011).

The effective pressure $\hat{N}$ differs from the overburden pressure P_0 depending on the basal water ~~content,~~ saturation fraction $s \in [0,1]$,

$$\hat{N} = N_0 \left(\frac{\delta P_0}{N_0} \right)^s 10^{\frac{e_0}{C_c}(1-s)}, \tag{3}$$

following the parameterization of Bueler and van Pelt (2015)~~:~~

$$\hat{N} = N_0 \left(\frac{\delta P_0}{N_0} \right)^s 10^{\frac{e_0}{C_c}(1-s)}.$$

~~The effective pressure decreases with increasing till saturation $s = H_w/H_{w,\max}$ to a minimum value of δP_0 at $s = 1$~~. The parameter ~~P_0 is~~ $\delta = 0.02$ is an empirical scaling factor of the overburden pressure~~, with $\delta = 0.02$ being an empirical minimum fraction~~. This means that the effective pressure at the base is equal to 2% of the overburden pressure ~~when~~ then the till is saturated, and any excess water is considered to be drained from the system (Bueler and van Pelt, 2015). The parameter $N_0 = 1000$ Pa is a reference pressure at a reference void ratio $e_0 = 0.69$, and $C_c = 0.12$ is the coefficient of compressibility of the till. Finally, since the overburden pressure is an upper limit for the effective pressure, the minimum of the two is taken,

$$N = \min \left\{ P_0, \hat{N} \right\}. \tag{4}$$

The basal water layer thickness H_w has a maximum value of $H_{w,\max} = 2$ m, and $s = H_w/H_{w,\max}$. In turn, H_w changes with the basal mass balance $\dot{b}_g$ and is removed via a constant drainage rate C_d,

$$\frac{\partial H_w}{\partial t} = -\frac{\rho_i}{\rho_w} \dot{b}_g - C_d, \tag{5}$$

where ρ_i and ρ_w are the densities of ice and water~~densities~~, respectively, and ~~$\dot{b}_g$ is the basal mass balance,~~

$$\dot{b}_g = -\frac{1}{\rho_i L} \left(Q_b + k \frac{\partial T}{\partial z}\bigg|_b + Q_\mathrm{r} \right). \tag{6}$$

The function $\dot{b}_g$ therefore converts the heat flux at the base to a melt rate via the latent heat of ice fusion, L. The heat flux consists of the heat generated by friction due to sliding of the ice along the base Q_b as well as the heat conducted into the column of ice above given by the coefficient of conduction of ice k and the temperature gradient of the ice at the base $\frac{\partial T}{\partial z}\big|_b$. In addition to this, there is a geothermal heat flux boundary condition Q_geo imposed 2 km below the surface and the heat diffuses vertically through the bedrock. The term Q_r is then the flow of heat into the ice at the interface of bedrock and ice. The isostatic adjustment of the bedrock under the ice sheet uses the elastic lithosphere-relaxing asthenosphere (ELRA) model (Meur and Huybrechts, 1996) with a relaxation timescale of 3000 years.

At the ice-sheet surface, Yelmo is coupled to REMBO (Robinson et al., 2010). REMBO is a two-dimensional model with vertically integrated equations for energy and moisture balance. These variables are diffused throughout the model domain to represent processes at the dominant synoptic scale. The strengths of this diffusion decreases with increasing latitude to represent decreased atmospheric activity at higher latitudes. REMBO also accounts for orography, whereby precipitation rates

increase as the horizontal surface gradient increases. The temperature and precipitation fields of REMBO are calculated at 100km resolution, and a bilinear interpolation is used to input these as boundary fields to the surface of Yelmo.

Ice sheets gain or lose mass through their surface mass balance (SMB), which is determined by the air temperature at the ice-sheet surface and precipitation rates calculated by REMBO. The SMB can be separated into a positive contribution from the precipitation and a negative contribution resulting from surface melt, M_s. The latter is calculated using an insolation-temperature melt method (ITM), whereby insolation S and albedo α_s are explicitly taken into account (Bintanja et al., 2002):

$$M_s = \frac{\Delta t}{\rho_w L_m}[\tau_a(1-\alpha_s)S + c + \lambda T], \tag{7}$$

where Δt is the length of a day in seconds, ρ_w is the density of water, and L_m is the latent heat of melting. The atmospheric transmissivity $\tau_a = 0.46 + 0.00006 z_s$ is a function of the surface elevation z_s, increasing melt with altitude and thereby acting as a negative feedback for large ice-sheet thicknesses. The surface albedo is calculated as

$$\alpha_s = \min\left(\alpha_g + \frac{d}{d_{\text{crit}}}(\alpha_{s,\max} - \alpha_g), \alpha_{s,\max}\right), \tag{8}$$

where $\alpha_{s,\max}$ is the maximum albedo of snow and α_g is the albedo of the ground, and $\frac{d}{d_{\text{crit}}}$ is the ratio of snow thickness d to a maximum value d_{crit}. Finally, c and λ are free parameters that fit surface temperature T to present-day melt rates of the GrIS Robinson et al. (2010).

2.2 Experimental setup and boundary conditions

~~The model is first run to equilibrium for 400 ka to arrive at an initial state (Fig. 1) corresponding to the~~

To investigate r-tipping of the GrIS, an equilibrated initial state is required. This allows us to disentangle any effects of inertia associated with transient systems approaching equilibrium from the r-tipping behaviour.

Instead, the present-day GrIS ~~. The~~ is initialized using ice-sheet thickness and bedrock topography ~~are initialized using~~ from the data from version 5 of the BedMachine mapping of Greenland (Morlighem et al., 2017) ~~. The surface boundary conditions of Yelmo are determined by REMBO, which uses~~ and the ERA-40 climatology (Uppala et al., 2005) as ~~its boundary conditions .~~ boundary conditions for REMBO, and allowed to relax to and equilibrium state over a 200 ka simulation. This equilibrated initial state is shown in Fig. 1, state A. A comparison of the surface velocities of this initial state to those of the present-day GrIS Joughin et al. (2018) are seen in Appendix Fig. A1 The states of the GrIS at ~~200 ka and 300~~ 300 ka and 400 ka are also saved as initial states B and C respectively, representing a small perturbation to the initial state at ~~400 ka. This is the starting point from which the model is forced in subsequent simulations.~~ 200 ka. The three initial states can be seen in Fig. A2 and a comparison of their ice thickness and surface velocities is found in Fig. A3. The use of an ensemble of multiple initial states is not common for ice-sheet simulations, but is implemented to test the robustness of the results and a possible dependence on initial conditions.

~~By definition, r-tipping occurs at a forcing temperature below the critical b-tipping value, so the latter must first be estimated. To estimate the bifurcation point of the GrIS, the sea-level summer air~~ The model is externally forced in subsequent experiments

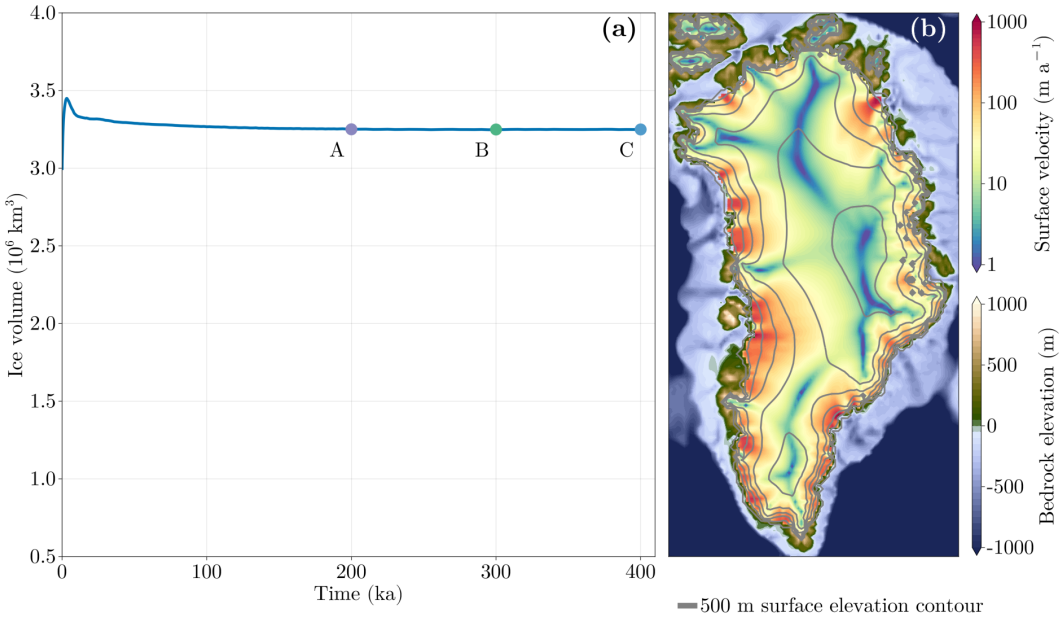

Figure 1. (a): Ice volume time series of the ~~equilibrium~~ spinup simulation~~for the~~ . The three initial states A to C are shown. (b): ~~Ice sheet extent~~ Surface velocity of the initial state C at the end of the 400 ka spin-up run.

by applying a constant summer temperature anomaly to the surface temperature and ocean temperature at the ~~boundaries of REMBO are gradually increased~~boundary of the model domain of REMBO, as in Gutiérrez-González et al. (2026) and Robinson et al. (2012). This regional summer temperature anomaly is approximately equivalent to a global mean temperature increase. ~~This forcing is applied using~~ Since r-tipping occurs at a forcing temperature below the critical b-tipping value, the latter must first be estimated. To this end, an adaptive quasi-equilibrium forcing (AQEF) function ~~starting at each of the three initial states. This AQEF interactively adapts the forcing in order to maintain~~ is used. The AQEF is a transient simulation whereby the forcing is increased in such a way that it is held constant while the ice sheet ~~in a quasi-steady state by ensuring that~~ is not in quasi-equilibrium, and is implemented as such: The GrIS is considered to be quasi-equilibrated when the rate of ~~ice-volume loss stays below a given threshold, equal to 2 gigatons per year averaged over~~ mass loss of the last 100 ~~years. The forcing increase is done~~ years of model time is less than this threshold, which is here taken as 2 Gt a^{-1}. While the ice sheet is not in quasi-equilibrium, the forcing is held constant. Once quasi-equilibrated, the forcing is increased in an adaptive way~~such that~~ : the longer it takes the model to ~~equilibrate~~achieve quasi-equilibrium, the less the forcing is ~~subsequently increased.~~ increased. The maximum rate at which the forcing can be increased is 10^{-5} K a^{-1}, and the minimum rate is 0. In this way, the forcing parameter does not increase while the ~~tipping is occurring~~collapse of the ice sheet is occurring, preventing rate-dependent hysteresis (An et al., 2021).

Once the ~~tipping~~ bifurcation point has been estimated, it is used to determine a range of parameters for the subsequent ramping experiments that are used to assess the possibility of r-tipping. In these ramping experiments, the forcing is increased at a linear rate to some value less than the ~~tipping~~ bifurcation point. Thereafter, the forcing is kept constant and the ice sheet is allowed to equilibrate over 400 ka. An ensemble of simulations is generated by applying different rates of increase and maximal forcing values, allowing the effect of the rate and magnitude of warming to be evaluated. These ramping experiments are also performed starting at each of the three initial states to investigate the effect of different initial conditions.

3 Results

3.1 Tipping of the ice sheet

Figure 2 shows the ice volume as a function of the forcing parameter, the regional summer temperature anomaly, for the three initial states. There is clear tipping behaviour for a forcing of +~~1.275~~ 1.28 K, which is essentially independent of the choice of initial state. This tipping resembles what is expected for a saddle-node bifurcation.

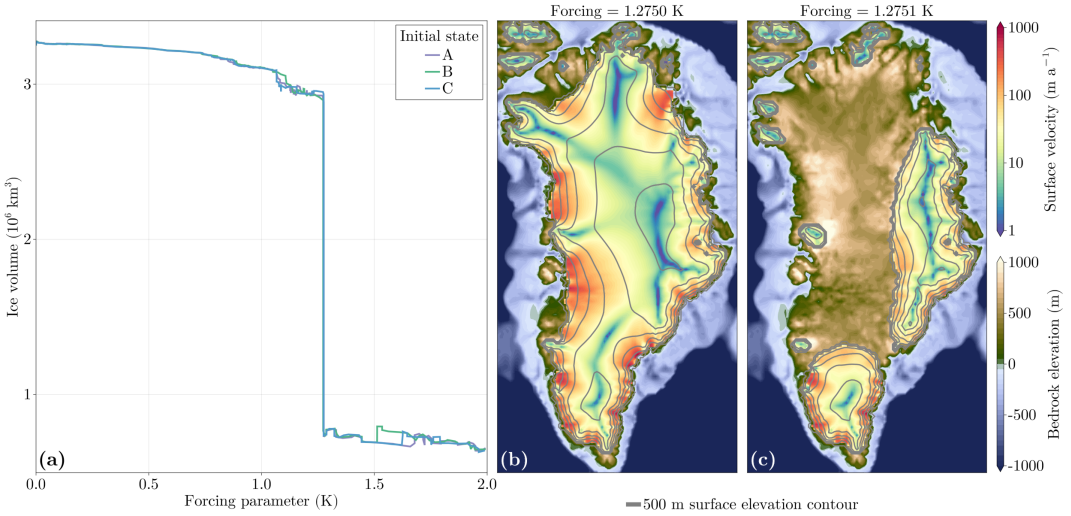

Figure 2. (a): ~~Equilibrium~~ Quasi-equilibrium ice volume of the GrIS as a function of the applied regional summer temperature anomaly in parameter space to estimate the ~~tipping~~ b-tipping value for initial states A to C. (b): Ice-sheet before tipping. (c): Ice-sheet after tipping.

The retreat of the GrIS during the tipping event is seen in Fig. 3. Spatially, the retreat begins in the north. Due to the similarities in the model setups between this study and that of Robinson et al. (2012), the spatial tipping pattern is equivalent. The pattern of ~~ice sheet~~ ice-sheet loss is also similar to that of Zeitz et al. (2022) (their Fig. 3a) albeit without the regrowth of the ice sheet.

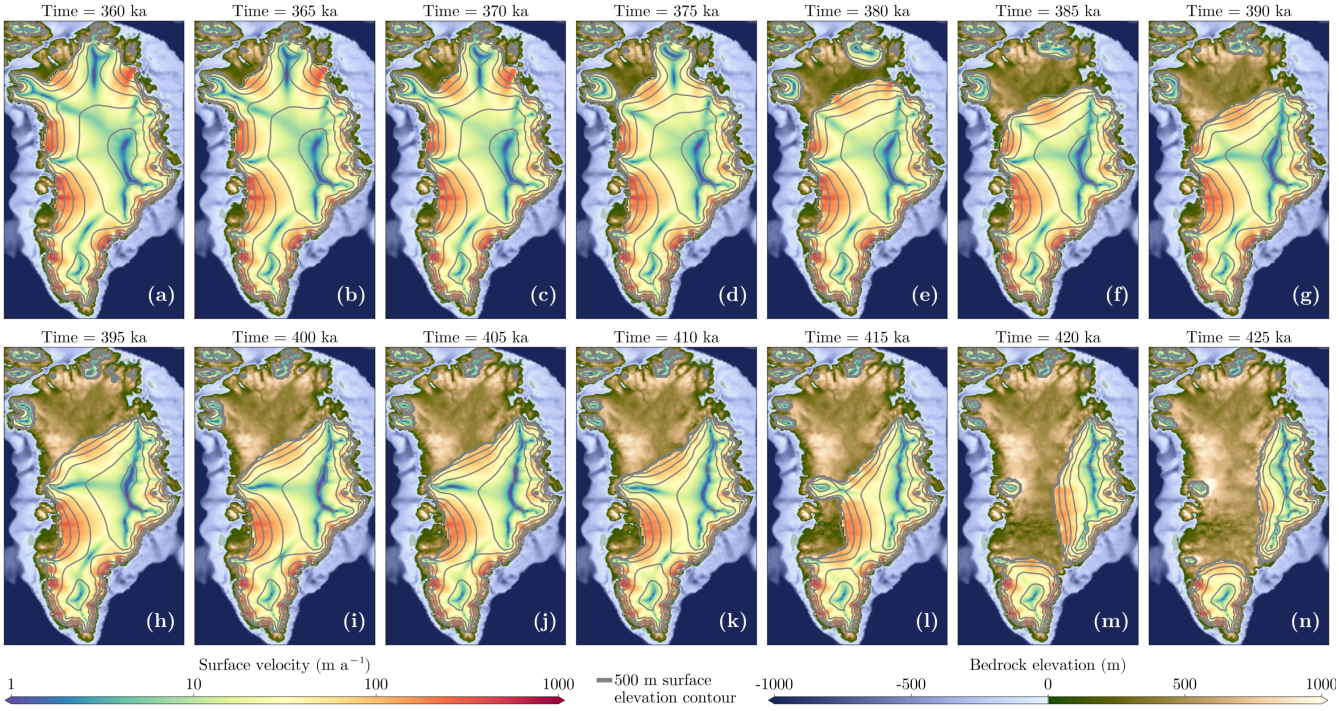

Figure 3. Ice extent and velocities during the tipping event at a fixed forcing value of +~~1.275~~ 1.28 K.

3.2 Ramping experiments

Since the ~~tipping~~ bifurcation point is located at +~~1.275~~ 1.28 K, the maximal forcing of the ramping experiments are chosen as +1.00, 1.05, 1.10, 1.15, 1.20, and 1.25 K. A value of +1.30 K past the ~~tipping~~ bifurcation point is also included to confirm that tipping does indeed always occur when forced past +~~1.275~~ 1.28 K. The forcing increases linearly at a rate of 10^{-1}, 10^{-2}, 10^{-3}, 10^{-4}, or 10^{-5} K a^{-1}, up to one of the seven maximal forcing values noted previously. The time series of the forcing is shown in Fig. 4. As each of these ~~120~~ ramping experiments is initialized from one of three states A, B and C, the entire ensemble consists of $7 \times 5 \times 3 = 105$ members ~~.~~ (Fig. 5.

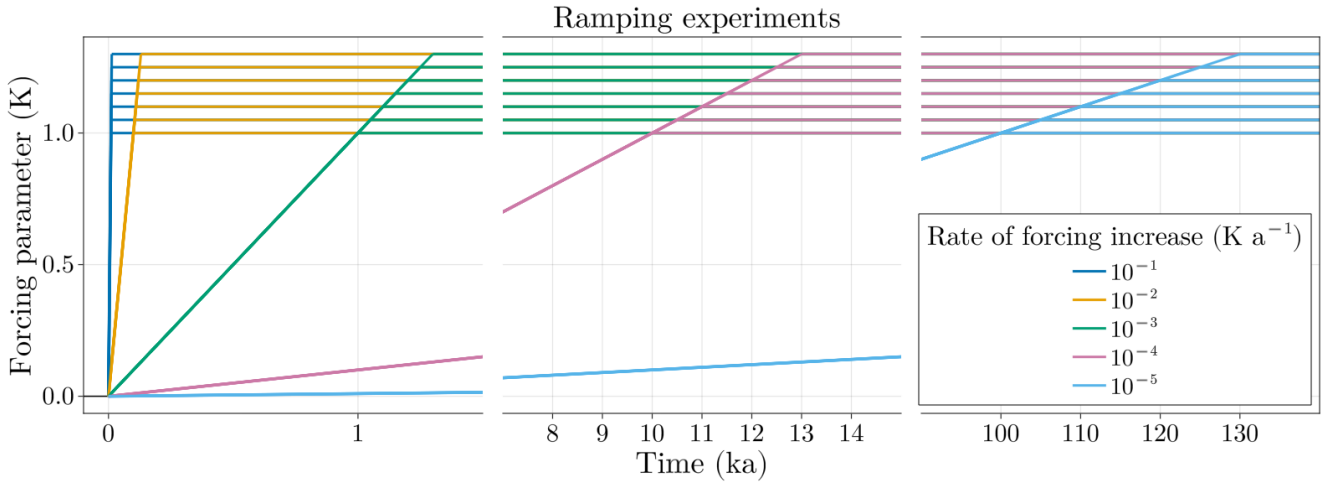

Figure 4. Time series of the forcing amplitude during the ramping experiments.

~~The simulations in Fig. 5~~

Figure 6 shows the tipping behaviour in the form of both the final volume and tipping time for each simulation. Figure 6 a) suggests rate-induced tipping. Tipping is observed for simulations forced to values lower than the critical value for b-tipping of +~~1.275~~ 1.28 K, occurring between +1.10 and +1.25 K. Tipping also occurs for all of the simulations forced past the ~~tipping~~ bifurcation point, that is, those forced to +1.30 K. What is absent, however, is some critical rate below which tipping does not occur, implying that r-tipping of the GrIS can occur even for very slow rates of forcing.

One prominent feature in this ensemble of simulations is the non-monotonicity in the ~~tipping times. There is some agreement in tipping times among a given initial condition, as well as a dependence of the mean tipping timeon the maximal forcing, being shorter for larger values. However, there is no clear relationship between the tipping time and the~~ time before the tipping occurs, hereafter referred to as the 'tipping time', with rate of forcing~~. Even for~~ , magnitude of forcing, and initial condition. For the same initial conditions, ~~sometimes~~ longer tipping times are ~~achieved at lower~~ seen for faster forcing rates. For instance, for initial condition C at a forcing level of +1.25 K~~(panel (m) of Fig. 5)~~, the trajectory forced at a rate of 10^{-2} K a^{-1} tips around 300 ka, where the trajectory forced at slower rate of 10^{-3} K a^{-1} tips earlier, around 100 ka.

In addition, tipping times for a maximum forcing of 1.30 K can be longer than those for 1.25 K. For example, for initial condition B and the slowest rate of 10^{-5} K a^{-1}, the tipping occurs around 250 ka for a forcing of +1.25 K and around 400 ka for +1.30 K~~(panels (m) and (n) of Fig. 5, respectively).~~ . Finally, even for the same magnitude of forcing and rate of forcing, the tipping times are not consistent over initial conditions. For example, ~~in panel (l) of Fig. 5, the simulation forced~~ the simulations forced to +1.20 K at a rate of 10^{-3} K a^{-1} tip at 300, 350 and 250 ka for initial conditions A, B and C respectively. Overall ~~, sensitive dependence on initial condition, indicative of chaos, appears to be affecting the outcome of the tipping~~the tipping behaviour seems to be sensitively dependent on the initial state of the system and the rate of forcing.

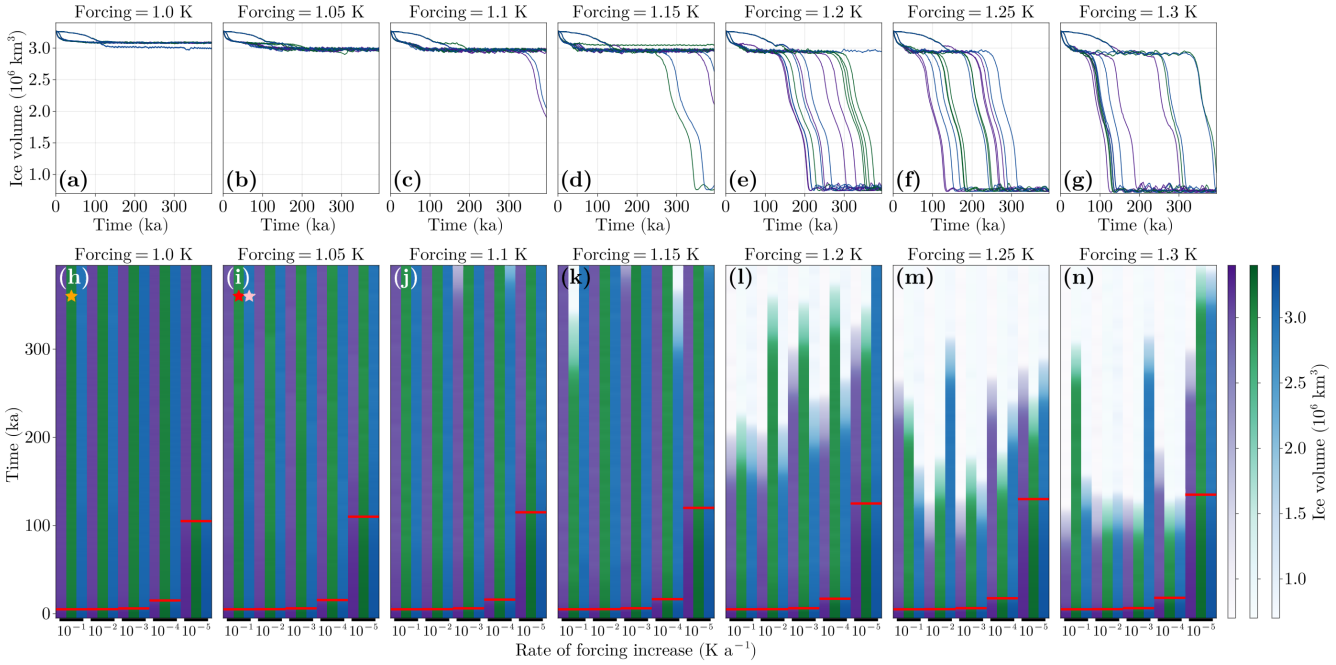

Figure 5. (a-g): Time series of the ice-sheet volume for all simulations to a given maximal forcing. (h-n): Time series of the ice volume for all of the simulations grouped by maximum forcing value. The initial state of each simulation is indicated by the different colours: purple for A, green for B and blue for C. For a given maximal forcing, the simulations are ordered along the bottom axis in decreasing rate of forcing, with the red line indicating the time where the forcing reaches its maximum. The stars indicate simulations that appear in Figs. 8-12 and B1-B3

~~(a-g): Time series of the ice-sheet volume for all simulations at a given maximal forcing. (h-n): Time series of the ice volume for all of the simulations grouped by maximum forcing value. The initial state of each simulation is indicated by the different colours: purple for A, green for B and blue for C. For a given maximal forcing, the simulations are ordered along the bottom axis in decreasing rate of forcing, with the red line indicating the time where the forcing reaches its maximum.~~

While investigating the cause of these random tipping times, irregular oscillations in the ~~ice sheet~~ ice-sheet volume before tipping were observed. These oscillations can be isolated to a single region of the ice sheet: the northwest drainage basin, where the ice-sheet also begins its retreat during a tipping event. It is hypothesized that the random tipping times are linked to these irregular oscillations. An example of the oscillations for each maximal forcing is shown in Fig. ~~6~~7. For all these simulations, there is an initial loss of mass during the first 50 - 80 ka of simulation time. Thereafter, for a maximal forcing of +1.00 K, there is a relatively small amount of variability around a steady ice volume of about 3.09 $\times 10^6$ km^3. For maximal forcing values between +1.05 and +1.15 K, the mean ice volume is lower, between 2.9 and 3.0 $\times 10^6$ km^3. The ~~variability is also larger in both amplitude and period~~ice sheet experiences fluctuations in volume with a magnitude on the order of 0.05$\times 10^6$ km^3 and

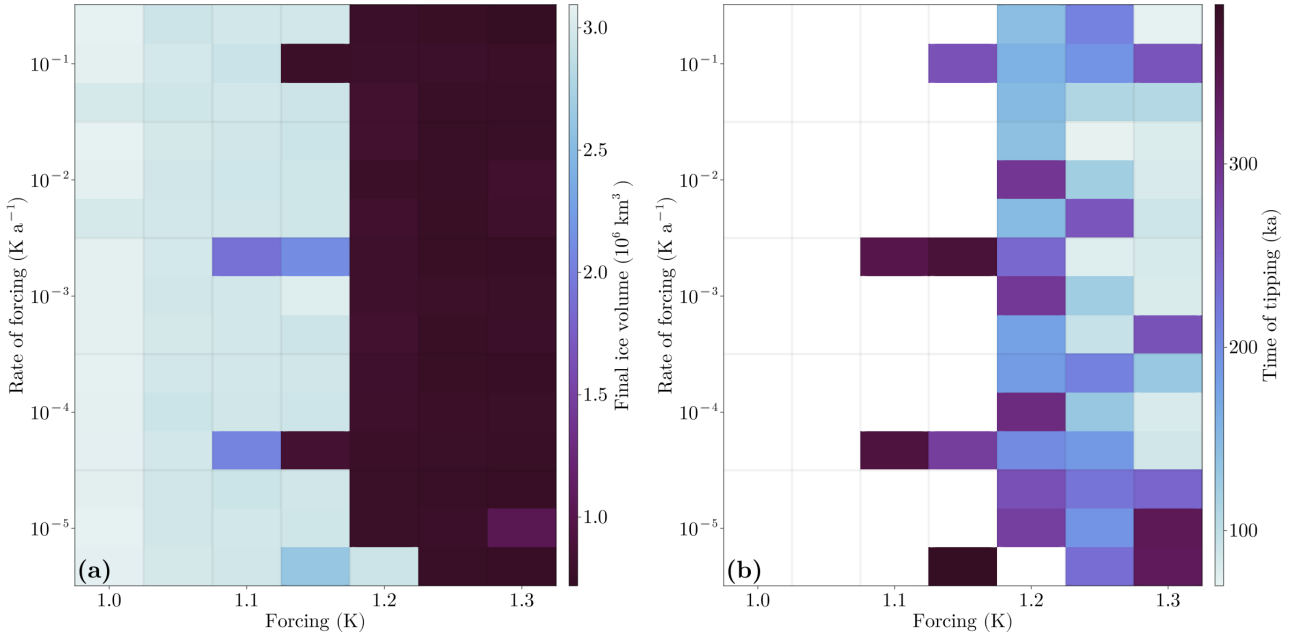

Figure 6. a): Final ice volume for each of the ensemble members, grouped by the three initial states, for each combination of magnitude and rate of forcing. b): As in a), but indicating the tipping time for each of the ensemble members, defined as the time when the ice volume decreases below 2.85 $\times 10^6$ km^3

a period between 8 and 30 ka. Finally, the simulations for maximal forcing of +1.20 to +1.30 K in Fig. ~~6~~ 7 retreat to a much smaller ice volume, representing a collapsed GrIS as seen in Fig. 2 ~~.e~~c).

3.3 Spatial and temporal behaviour of the oscillations

Two simulations at a forcing of +1.00 and 1.05 K are compared, as this represents the onset of the large-amplitude variability seen in Fig. ~~6~~7. Further examination of the oscillations show they are a result of two ice streams that alternate between periods of stagnant and rapid basal sliding. These are the Humboldt and Petermann glaciers, which lie in close proximity to each other on the northwestern ice-sheet edge ~~.~~(Fig. 8). These glaciers are both regions of fast-flowing ice (Carr et al., 2015; Ehrenfeucht et al., 2023; Hillebrand et al., 2022) and behave as ice streams in the model simulations. In the model, ice streams can be identified by grounded ice with a significant basal velocity.

The first difference to be seen is the extent of the ice sheet in this region. For a forcing of +1.00 K, the ice-sheet margin is such that the Humboldt ice stream (HIS) is marine-terminating, with the Petermann ice stream (PIS) covering the Petermann fjord. The ice sheet in this case is termed ‘unretreated’. In the simulation with a forcing of +1.05 K, the ice sheet extent is much reduced. From the mean ice-thickness profiles, the ice margin is almost 100 km further inland (panels a, c, d and f of

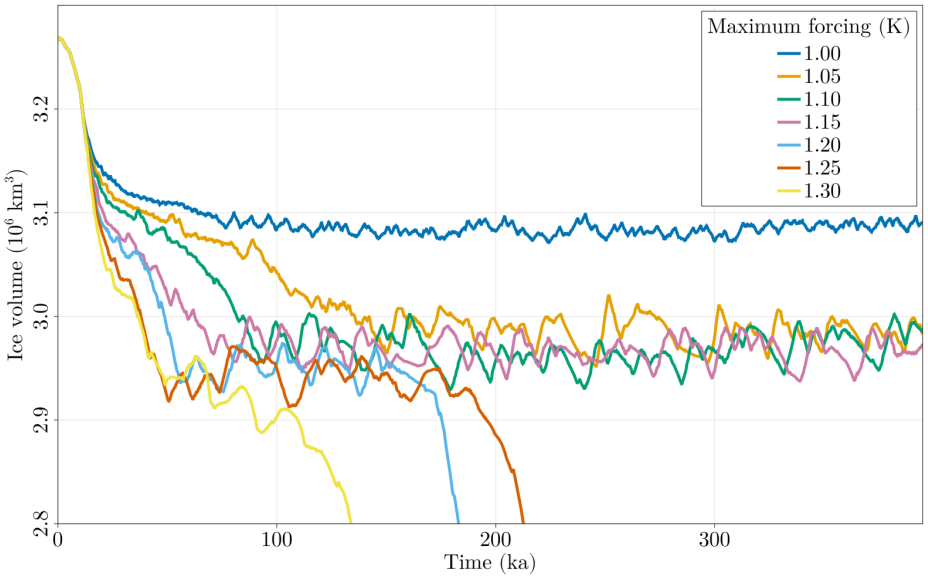

Figure 7. Time series of ice volume for simulations from Fig. 5 for initial condition A, rate of warming 10^{-4} K a^{-1}, and a range of maximal forcing values.

Fig. ~~7~~8). The HIS is no longer connected to the ocean, although the PIS terminates at the Petermann fjord. We refer to this as the 'retreated' configuration, with the two separate ice streams being designated the retreated HIS and retreated PIS.

The temporal behaviour of the two ice sheet extents is compared by taking the spatial mean in two grid boxes, one containing the PIS/retreated PIS and the other the HIS/retreated HIS, as seen in panels (a) and (j) of Fig. ~~8~~9. For the unretreated case, the basal velocities in the two different ice streams behave quite differently. The PIS is in a state of steady flow of around 100 m a^{-1}, facilitated by a constant basal water layer thickness. The HIS, in contrast, alternates between near zero basal movement and sliding velocities of 100 m a^{-1}. The periods of stagnation are due to an increase of basal friction because of a reduction in the water content of the till due to freezing or drainage. While the basal velocities are minimal, the ice thickness increases, establishing a 'build up' phase. The subsequent loss of mass due to rapid ice streaming is a 'surge' phase. The period of these oscillations varies between approximately 5 and 9 ka. This steady cycle of mass gain during the build-up phase and loss during the surge results in an oscillation in mean ice thickness between 100 and 200 metres. The PIS also shows a smaller alternation in ice thickness with a similar temporal pattern while maintaining constant ice-stream flow, suggesting the thickness variations are influenced by the oscillations of the nearby HIS.

In the retreated configuration, the oscillations of ice thickness and basal velocity have larger amplitude and periodicity, as mentioned previously. While the exact location of the retreated PIS and retreated HIS differs slightly in all the simulations showing oscillations, their existence is robust among the ensemble. In contrast to the unretreated PIS, the retreated PIS is no longer in a steady-flow state and instead displays the same build-up/surge variability as the ~~HIS~~ unretreated and retreated HIS.

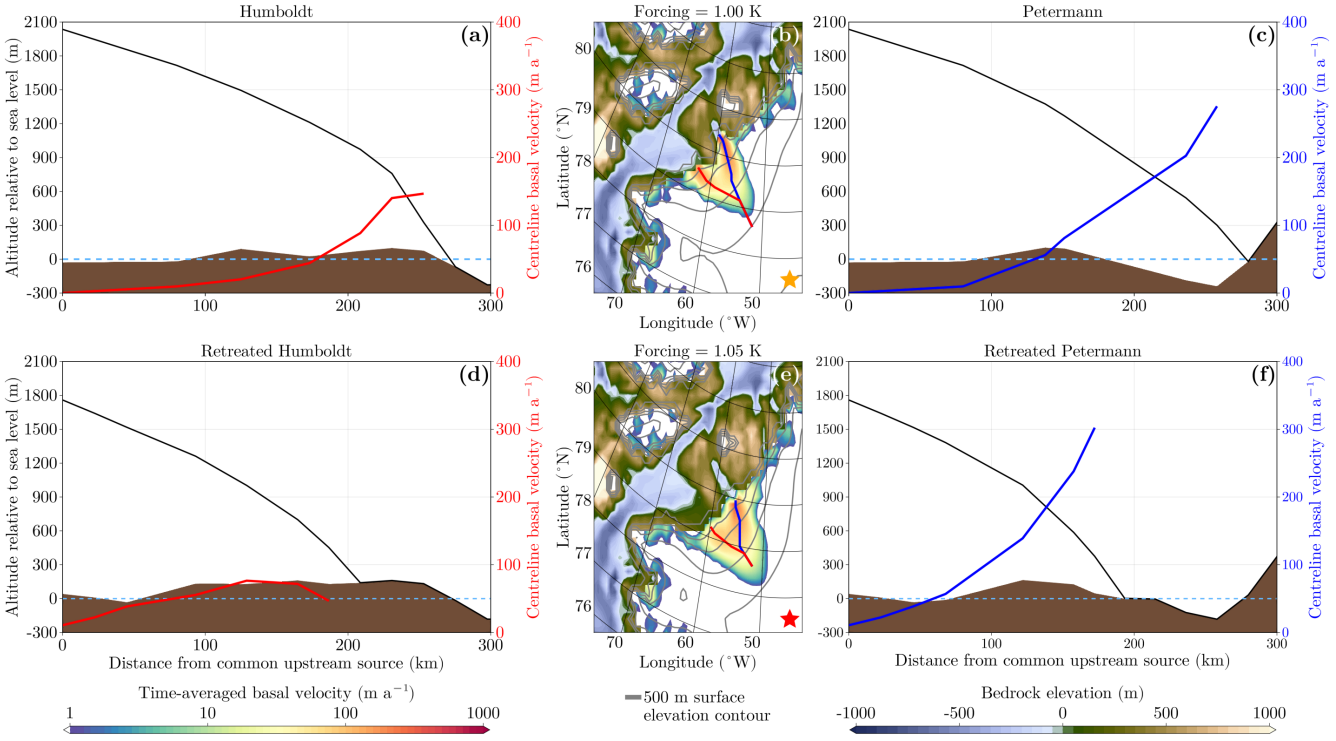

Figure 8. (a), (c): Centreline ice-thickness profile (black) and basal velocities along the centreline for the HIS and PIS. (d), (f): same as (a), (c) but for the retreated HIS and retreated PIS. (b), (e): time-averaged basal velocity field. The lines perpendicular to the grey height contours are the ice-stream centrelines for Humboldt (red) and Petermann (blue).

Two broad patterns for the oscillations of the retreated ice extent emerge. The first is one of a long, asymmetric build-up and surge event. An example is seen around 225 to 260 ka in panels c, e, g and i of Fig. ~~8~~9. While the basal velocity in retreated PIS switches abruptly between the build-up and surge phases, the increase of the basal velocity in the retreated HIS is gradual. This ~~slows~~ accelerates the mass loss until a point where the basal water layer thickness rapidly decreases in both ice streams when the ice thickness reaches its minimum, due to the thermomechanical coupling . The second pattern is that of short oscillations with a period of around 8 ka. These are seen in the last 60 ka of the time series in the panels c, e, g and i of Fig. ~~8~~9. The basal velocity in retreated PIS abruptly switches between maximal and minimal, with corresponding drops in basal water-layer thickness when the velocity is near zero. In retreated HIS, the till remains saturated with water. However, the basal velocity and thereby the flow is not steady. It increases during the surge and decreases during the buildup of the nearby retreated PIS. This indicates an influence of the retreated PIS on the retreated HIS. The magnitude of ice-thickness change during this pattern is not as large as for build-up and surge variability, being around tens of metres per year in the spatial mean.

Thus the distinguishing factor between the two patterns is that during the short oscillations, the retreated PIS is in a build-up/surge mode~~and~~ , whereas the retreated HIS has a constant till saturation~~associated with steady flow but experiences~~ . This

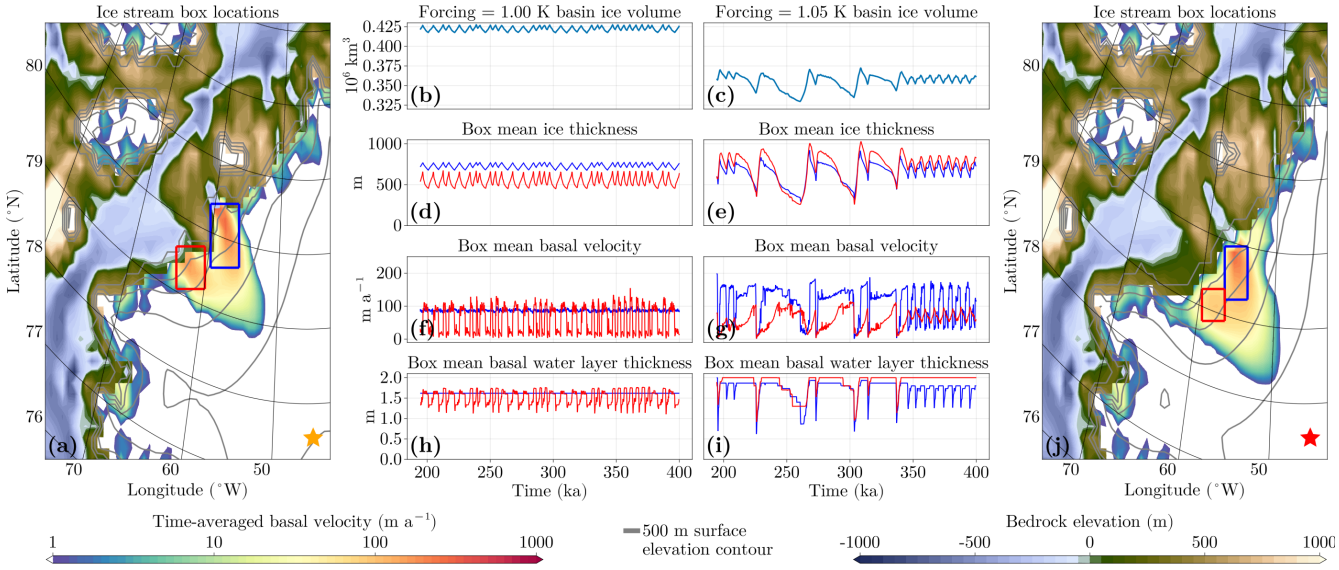

Figure 9. (a), (j): Location of the PIS/retreated PIS (blue) and HIS/retreated HIS (red) ice-stream boxes superimposed over the temporal average of the basal velocity ~~during the oscillations~~ between 200 and 400 ka of the unretreated (a) and retreated (j) configurations. (b-i): Time series of basin ice volume, mean ice thickness, basal velocity, and basal water content in the ice-stream boxes in the unretreated (d, b, f, h) and retreated (c, e, g, i) configurations.

causes the retreated HIS to be in a steady-flow state, while still experiencing small oscillations due to the proximity to the retreated PIS. On the other hand, both the retreated HIS and the retreated PIS are in the build-up/surge mode during the longer-period events. ~~Additional~~ In addition to these modes, in some simulations with these oscillations there is occasionally a period where both retreated HIS and retreated PIS are in a steady flow state with intermediate mean basal velocities of around 100 m a^{-1}, with an associated minimum in the ice volume which may last tens of thousands of years~~.~~, as seen in Fig. 10

The differences between the behaviour of the PIS and HIS in both configuration can be explained by slight variations in their topography and forcing fields, as seen in Fig. 11. The constant geothermal heat flux in the PIS is slightly larger than in the HIS with a spatial average of 48.75 and 48.25 mW m^{-2}, respectively. During the periods where oscillations occur, the basal mass balance in the PIS varies much more than in the HIS, primarily due to the larger frictional heating (Q_b in equation 6) which is a direct result of larger basal velocities in the PIS while it is streaming (Fig. 11, panel g). The bed elevation of the HIS is lower than the PIS, leading to lower average basal friction and thereby making it more prone to the steady-streaming state as opposed to occasional refreezing. Finally, the HIS receives more precipitation than the PIS on average, about 0.28 m.w.e a^{-1} compared to 0.26 m.w.e a^{-1}, respectively. This might allow for the mass lost by the HIS during streaming to be better balanced by the accumulation, as opposed to the PIS, where lower accumulation means the ice thickness can only regrow once the streaming has quiesced.

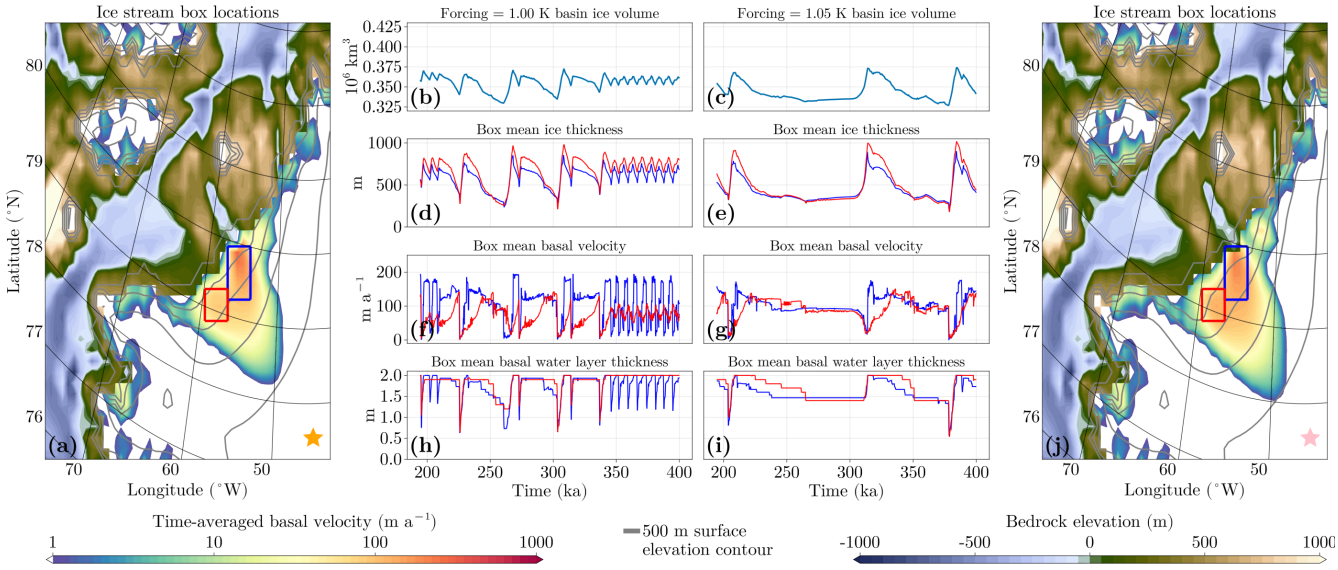

Figure 10. As Fig 9, but starting at initial state C instead of B.

3.4 Effect of glacial isostatic adjustment on the oscillations

The glacial isostatic feedback has been demonstrated to cause oscillations in ice sheet volume (Petrini et al., 2025; Zeitz et al., 2022) , and the relaxation time of 3000 years is relevant on the timescales of the observed variability in the HIS and PIS. Figure 12 shows the magnitude of variation in the altitudes of the bedrock and ice-sheet surface as well as the ice thickness. The maximal uplift of the bedrock in both the HIS and the PIS is 40 metres, which occurs during a long surge event (between 230 and 260 ka in Fig. 12). During this time, the decrease in ice thickness is about 600 metres for the HIS and 500 metres for the PIS. So, while there is some effect of the GIA, the magnitude of the uplift of the bedrock is never so large as to affect the build-up/surge variability of the ice sheet. If the regrowth of the ice sheet after a surge were triggered by the GIA bringing the bedrock to an altitude that allows for a positive SMB, we may expect to see a period of minimal ice thickness during which the bedrock is uplifting, and at a certain altitude the ice thickness to start increasing again. Instead, we see the GIA simply lagging the ice thickness. The ice regrowth instead corresponds to a minimal basal velocity, i.e. an end of the surging. It may be the case that the GIA contributes to the maintaining of the oscillations by adding some altitude to the ice surface, but it does not set the pace of the oscillations.

3.5 Removal of the oscillations

To asses whether the lack of predictability of the tipping is due to ice-stream oscillations or otherwise due to other factors, we change the parameterization of the ice streams to eliminate their ability to oscillate and investigate the consequences. As described previously, the ice-stream oscillations are surges in the basal velocity of the ice stream due to the thermomechanical

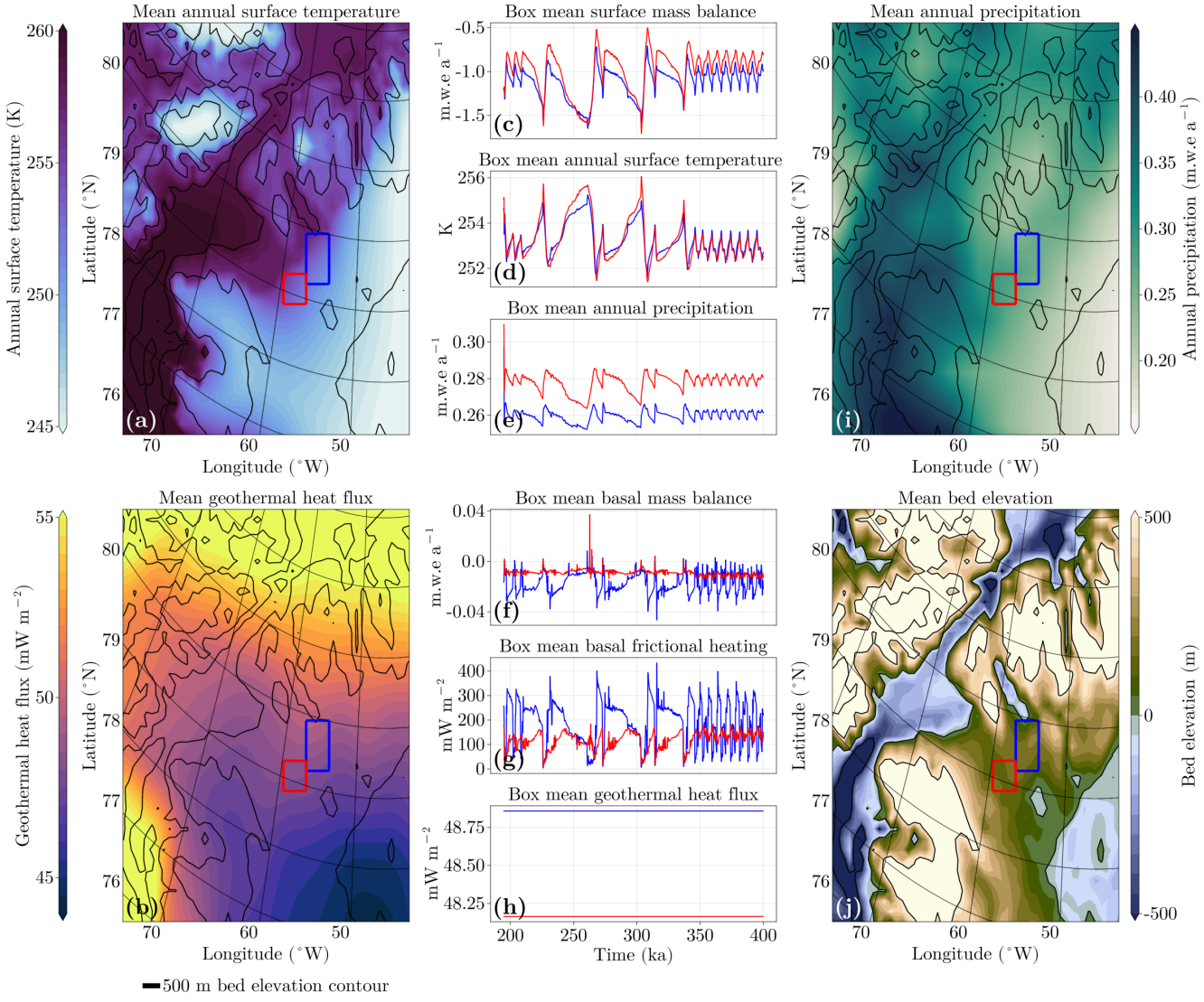

Figure 11. (a), (e): Location of the retreated PIS (blue) and retreated HIS (red) ice-stream boxes superimposed over the temporal average of annual surface temperature (a) and annual precipitation (e). (b-d): Time series of surface mass balance (b), annual surface temperature (c), and annual precipitation (d) in the ice-stream boxes.

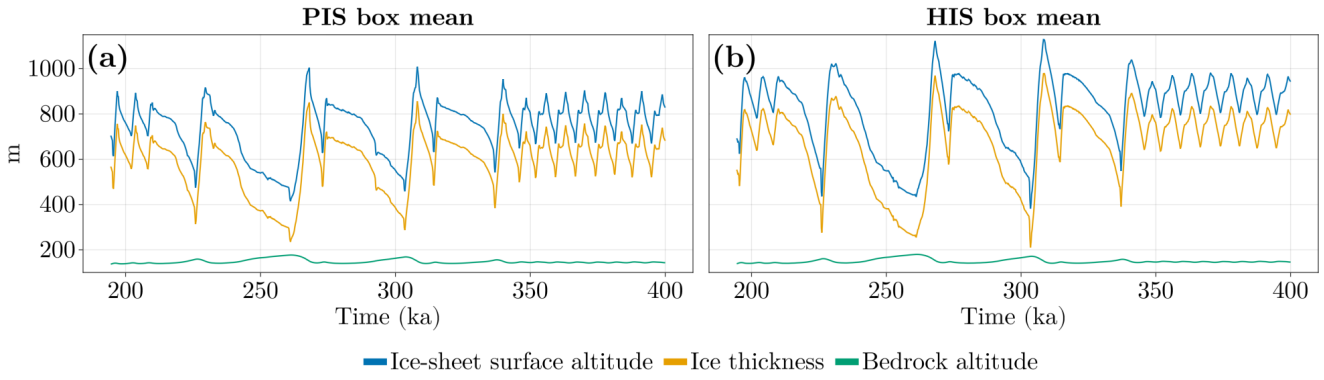

Figure 12. Ice-sheet surface altitude, ice thickness, and bedrock altitude in the retreated HIS and PIS boxes

coupling at the base of the ice sheet. To remove the oscillations but maintain the ice stream, the basal velocities in the region of interest need to be lower but non-zero. For lower basal velocities, the mass lost due to streaming is closer to the accumulation rate, bringing the ice stream to a steady flow state (Robel et al., 2013). To achieve this, the value of δ in Eq. 3 is increased. This raises the minimal effective pressure (Bueler and van Pelt, 2015) and thereby increases the basal frictional stress.

Increasing the value of δ and thereby the basal frictional stress has the effect of making the entire ice sheet less dynamically active, reducing the amount of mass loss due to ice streaming and calving. This means that the temperature forcing required to induce the collapse of the ice sheet is greater for larger values of δ.

Simulations with the original value of δ = 0.02 as well as increasing values of δ to 0.04 and 0.10 are shown in Fig. ~~9~~13. As δ is increased, we note an increase in the oscillatory period until the oscillations disappear completely. As this value affects ice streams across the entire ice sheet, the ~~tipping points~~ bifurcation point for each of these parameter values is different. Specifically, the ~~tipping~~ bifurcation point increases as δ increases, as the ice sheet is losing less mass due to lower ice stream velocities.

For $\delta = 0.02$, all (no) simulations with the strongest (weakest) forcing tip, but for intermediate maximum forcing values the tipping times do not decrease monotonically with the forcing rates. For a large enough value of δ=0.1, the ice-stream oscillations disappear and the tipping time for a maximal forcing of +2.10 K occurs at approximately the same time for each rate. That is, the dependency on the forcing rates disappears and the tipping is much more predictable. This suggests that the ice-stream oscillations introduce a delay in the tipping.

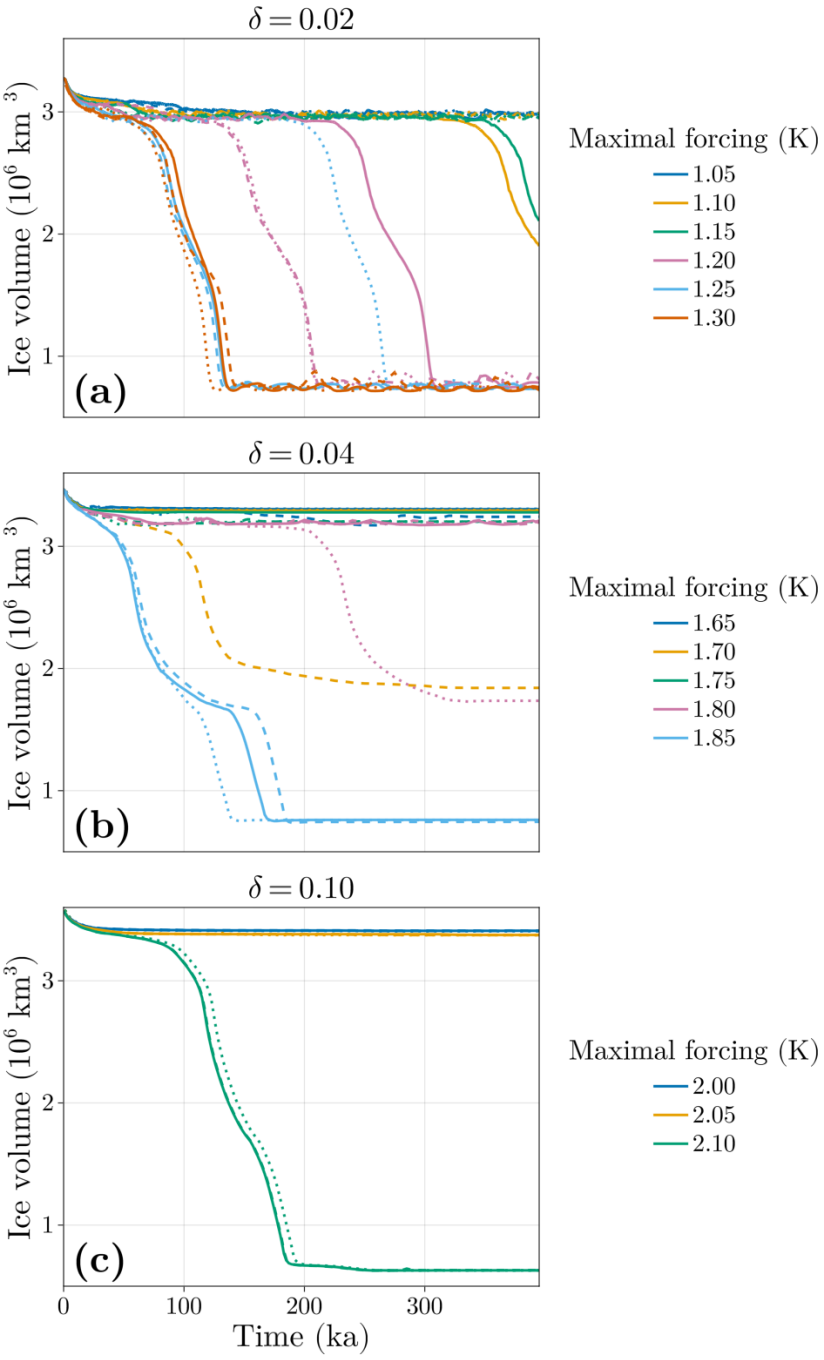

Figure 13. Time series of the ice sheet volume for increasing δ. For each value of δ, a range of forcing magnitudes at three rates starting from initial state A were applied: 10^{-1} (dotted lines), 10^{-2} (dashed lines) and 10^{-3} (solid lines) K a^{-1}.

4 Discussion

4.1 Ice-stream oscillations

Ice streams not only represent a mechanism of rapid mass loss in ice sheets, but have also been shown to be a source of internal periodic variability in models. Periodic behaviour of ice masses can be seen in glaciers that are confined to some topographical valley and/or have a basal slope, see for example Budd (1975); Kamb et al. (1985); Clarke (1987). Their reduced spatial extent also means their periodic behaviour is on a much shorter time scale of decades to centuries and thus directly observable. ~~Models show that ice sheets and ice streams , similar to valley glaciers, can also exhibit oscillatory behaviour under the right conditions.~~

However, present-day ice streams have been demonstrated to be accelerating (Catania et al., 2012) or decelerating (Beem et al., 2014; Ca , due to thermomechanical coupling at the base of the ice sheet, see also Scambos et al. (2017). Studies of oscillatory behaviour in ice sheets include parameterized models (Oerlemans, 1983; Fowler and Johnson, 1996; Payne, 1995; Robel et al., 2013) and comprehensive ice-sheet models with both idealized geometries ~~(Calov et al., 2010; Van Pelt and Oerlemans, 2012; Feldmann and Leverma~~ (Calov et al., 2010; Feldmann and Levermann, 2017; Hank et al., 2023; Sayag and Tziperman, 2011; Souček and Martinec, 2011; Van Pel and realistic topographies ~~(Papa et al., 2006; Roberts et al., 2016; Schannwell et al., 2023)~~(Hank and Tarasov, 2024; Papa et al., 2006; Rob . Additionally, some studies include a coupling to additional components of the climate system (Calov et al., 2002; Ziemen et al., 2019). Similarities between the oscillations seen in this paper and those observed in paleoclimate modelling studies are discussed in Appendix ~~A~~C.

~~Common to these studies~~ An important caveat of the results of this paper is that oscillations in the model are highly sensitive to the basal friction parametrization. The physical mechanisms at the base of the ice that allow for ice streaming are not perfectly understood, and therefore the behaviour of ice streams in models can depend heavily on the specific parameterization (Brondex et al., 2017, 2019). In situations where ice streams are marine-terminating, buttressing of ice shelves can serve to regulate the pace of mass loss, and thus decrease their sensitivity to the basal friction (Sun et al., 2020; van den Akker et al., 2026) . Due to the lack of floating ice shelves that might provide buttressing in the HIS and PIS, it can be understood that the oscillations are highly sensitive to the basal parameterization. Indeed, this is also reflected in the results of changing the parameter value of δ in section 3.4, which is further discussed in section 4.3.

Common to ice-sheet modelling is the use of a single initial state for a given combination of parameters rather than an ensemble. The use of an ensemble of states for investigating the evolution of an ice-sheet model is not too common, appearing in the studies of Tsai et al. (2017) and Verjans et al. (2025) to be able to account for the variability of the atmosphere and ocean when forcing the ice sheet. This is distinct to the results of this study, where the model is not coupled to an external climate model beyond a simple, deterministic diffusive energy and moisture balance atmosphere and thus the variability is internal to the ice sheet itself. As a result of using an ensemble, we see simulations at a given forcing magnitude exhibit significant deviations from each other, indicating a sensitive dependence on the initial state which is a hallmark of a chaotic mode of internal variability.

~~The chaoticvariability has an undeniable~~ While it is outside of the scope of the present study to formally prove that this mode of variability is indeed chaotic, some attempts may be made. Figure 14 shows, through a return mapping of subsequent peaks in the ice-sheet volume in the north-west basin, that the variability for forcing magnitudes of +1.05 K and above does not correspond to a simple 2-period cycle as it does for a forcing of +1.00 K. Two anomalous simulations are seen in the figure, one at a forcing of +1.00 K and one at +1.15 K, and are discussed in Appendix E. There are some features that can be explained under this chaotic framework, most notably the effect on the tipping behaviour. In particular, the unpredictable tipping times can be explained as being due to *chaotic transients*, which are described in ~~Appendix B~~Section 4.3. Whether the chaos is a genuine physical phenomenon or simply a result of parameterization is under contention and will require further investigation. As variability of this type has been reported in many other ice-sheet modelling studies, its existence is not entirely unfounded. What is unique to this study is the period and amplitude of the oscillations in Greenland, as well as its switching between two different modes due to a coupling of nearby ice streams. ~~While~~ The study of Kypke et al. (2025) examines this variability using a simplified model, establishing that this chaos can arise in a system with no spatial extent.

Large-scale oscillations in the GrIS ice volume have been reported in the modelling ~~study of Zeitz et al. (2022) , the period and amplitude~~ studies of Zeitz et al. (2022) and Petrini et al. (2025), but the characteristics of those oscillations are an order of magnitude higher than what is seen in the present work~~. This is due to the fact that glacial isostatic adjustment, which acts on a longer timescale than the~~ , having periods over 100 ka and amplitudes between 0.4 and 2.1 $\times 10^6$ km^3. The values of mantle viscosity and atmospheric lapse rate used in Yelmo and REMBO are 1×10^{21} (Pa s) and 6.5 (K km^{-1}) respectively, which places it in the oscillatory regime of Zeitz et al. (2022) under moderate temperature forcing. As all three models use an ELRA model of glacial isostasy, the primary difference between the observed behaviour in those studies compared with the present work is the regional atmosphere model. In Zeitz et al. (2022), the SMB is calculated using a positive degree day (PDD) method, which depends on the surface temperature, that is calculated locally as a function of the altitude. In Petrini et al. (2025), the SMB is calculated offline using the Community Earth System model, and then adjusted via a lapse rate during the runtime of the ice sheet model to reflect changes in ice sheet topography. However, there is no back-coupling of the ice sheet to the atmosphere. In contrast, REMBO allows for diffusion of energy and moisture, which decreases the local strength of the melt-elevation ~~feedback, plays a much larger role in their model .~~ feedback, thereby also reducing the sensitivity to the GIA feedback.

4.2 R-tipping of the GrIS

Accelerating mass loss is typically seen in marine-terminating outlet glaciers due to their sensitivity to oceanic forcing ~~(Howat et al., 2008; Krabill et al., 2004; Rignot and Kanagaratnam, 2006)~~(Choi et al., 2021; Greene et al., 2024; Millan et al., 2023; Rign
, suggesting rate-induced effects may be more prevalent in these areas due to the fast timescale of the marine ice sheet instability (Feldmann et al., 2025; Schoof, 2007; Swierczek-Jereczek et al., 2025; Weertman, 1974). However, they are ~~topographically confined and their impact~~ strongly controlled by their bed topography which only extends tens of kilometres from the coast, and while they experience rapid and significant decreases in their volume and are very relevant in the near future, their response may be limited ~~under greater forcing~~ over longer time scales (Joughin et al., 2010). For this reason, future loss due to negative ~~surface mass balance~~ SMB forced by increasing atmospheric temperatures could outweigh that of ice-sheet dynamics (Bevis

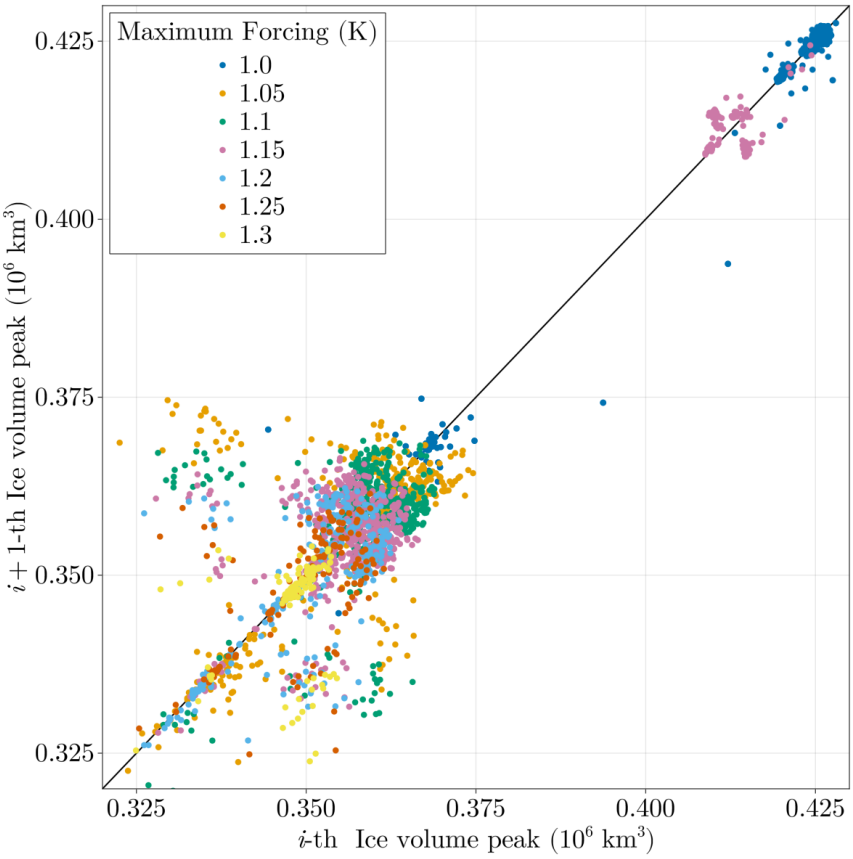

Figure 14. Return map of subsequent peaks in ice volume in the northwest drainage basin of the GrIS during surges.

et al., 2019; Enderlin et al., 2014). In addition, atmospheric forcing may be more critical in the north of Greenland compared to the south (Slater and Straneo, 2022). The ice extent shown in Fig. 3 indicates that the mass loss does not start in regions with many marine-terminating outlet glaciers, specifically the southeast (Van Den Broeke et al., 2009). In fact, many remain after the tipping has completed. This indicates that the possibility of r-tipping of the GrIS primarily by oceanic forcing may not be relevant.

The remainder of the ice sheet interacts predominantly with the atmosphere, and the mass loss occurs either through surface melt or dynamically through ice streams which may not necessarily be marine-terminating, meaning the activation of ice streams does not depend on oceanic basal melting. The question of whether the large-scale mass loss of the GrIS can be influenced by the sensitivity of these fast-moving ice streams to the rate of atmospheric warming is greatly obscured by the chaotic variability seen in the model. The simulations indicate that the tipping behaviour is affected by the rate of forcing but in a non-monotonic manner. There is no clear critical forcing rate for which r-tipping occurs, at least not for a rate faster than ~~one Kelvin~~ 1 K of warming over 100 ka. However, the long tipping times are not explained by non-monotonic r-tipping, as we

would expect any tipping events to occur at roughly the same time at a given forcing magnitude. That is, it is valid to claim that r-tipping does indeed occur since the final state of the GrIS depends on the rate of forcing in some way and it occurs before reaching the bifurcation point, but it is not the typical r-tipping as understood in simple non-chaotic systems. It is rather related to sensitive dependence on an initial state rather than any critical rate of forcing, with the different rates of forcing essentially being perturbations of the initial state, resulting in trajectories with unpredictable behaviour.

4.3 Chaotic transients

When the system transitions from one stable state to another, it can happen that it is trapped for a very long time in a complex saddle, which is stable in some directions and unstable in other directions. The time trapped shows sensitive dependence on the initial condition, which is a characteristic of chaos though the system eventually ends up in a predictable state. The trajectories are called *chaotic transients* (Lai and Tél, 2011). The long and unpredictable tipping times seen in this study are proposed to be due to such chaotic transients, and they can obscure the detection of r-tipping. The interplay between chaotic transients and r-tipping has been previously reported in a study by Lohmann and Ditlevsen (2021) for the AMOC. In their study, trajectories forced at different rates are brought close to the basin boundary between the stable 'AMOC on' state and the chaotic saddle that separates it from the stable 'AMOC off' state. This basin boundary is fractal, such that different rates of forcing may land the system differently on the saddle, where it experiences a chaotic transient such that the transitions to the AMOC off state is non-monotonic in rate. Alternatively, chaotic transients can arise due to a 'ghost attractor' that appears for forcing values just past a bifurcation point, where the drift away from the state, which is now no longer a stable fixed point, is slow (Strogatz, 1994). The oscillatory behaviour of the build-up/surge variability can generate unstable periodic orbits that 'collide' with the ice-covered GrIS attractor at the bifurcation point, generating the ghost attractor. The chaotic transients in this study may either arise when crossing a chaotic saddle before the bifurcation point due to r-tipping, or being caught in a ghost attractor after passing a bifurcation point due to b-tipping.

To answer the question of whether the GrIS experiences r-tipping in the ramping experiments, we must examine the chaotic transients. The critical forcing value was estimated as +1.28 K, and multiple simulations were observed to experience tipping for a forcing value less than this but with a fast rate of change of the forcing, implying r-tipping. However the adaptive quasi-equilibrium forcing itself may exhibit a chaotic transient, which would result in overestimation of the bifurcation point. Comparing the simulations ramped to +1.25 K (below the assumed critical value) and +1.30 K (above the assumed critical value), we notice that they are similar in oscillatory amplitude and period before tipping. If the oscillations are due to crossing a chaotic saddle before the assumed bifurcation point of +1.28 K, and therefore r-tipping, then they must be qualitatively different from the behaviour of the system after the bifurcation point is passed. But since the variability of the simulations at the two forcing values are qualitatively similar in period and amplitude, we conclude that they are generated by similar non-attracting sets (Lai and Tél, 2011). This implies that the critical value is not as assumed between +1.25 K and 1.30 K. Similar reasoning can be applied to all parameter values that result in tipping (i.e. +1.10 to +1.30 K). Thus, either the bifurcation point is between +1.05 K and 1.10 K and all transients are due to a ghost attractor, or the bifurcation point is larger than +1.30 K and all of the transients are due to an r-tipping through a chaotic saddle.

The behaviour of the chaotic transients in the present study more closely resembles those due to a ghost attractor after a bifurcation than due to r-tipping through a chaotic saddle. First, scaling laws indicate that the lifetime of the chaotic saddle, and thereby the tipping time, should increase as the maximal forcing approaches the bifurcation point (Mehling et al., 2024). In contrast, the mean lifetime of the chaotic transients, $\langle\tau\rangle$, scales with the magnitude of the parameter p past the crisis value p_c (Grebogi et al., 1986),

$$\langle\tau\rangle \sim (p - p_c)^{-\gamma}, \tag{9}$$

where γ is system-specific parameter value. This scaling of the tipping times mirrors the pattern seen in Fig. 5. Secondly, if r-tipping was present, we may expect to see tipping not occur below some critical rate, which is absent in the rates examined in this study. While it is not possible to evaluate the limit of the rate going to zero in finite simulation time, the rates investigated cover a wide range of physically realizable values. As the lowest rate of 10^{-5} K a^{-1} acts over the same time span as changes in orbital forcing, rates slower than this are not relevant.

4.4 Removal of the oscillations

Removing the oscillations by increasing δ makes the tipping more predictable. At a value of δ = 0.1, the tipping occurs at approximately the same time for both the fast and slow rates of forcing increase. This is in contrast to the simulations with δ = 0.02, where oscillations are present and the tipping at a given maximal forcing can vary by tens to hundreds of thousands of years depending on the rate and in a non-montonic manner. This corroborates the hypothesis that the oscillations cause the delay in tipping. For an intermediate value of δ = 0.04, tipping to an ice-free state only occurs for the largest forcing magnitude of +1.85 K. Interestingly, two simulations at lower forcing magnitudes see a tipping to an intermediate ice-sheet state. Such a state has been seen before in studies such as Ridley et al. (2010) and Robinson et al. (2012), but is not explored further in the present paper.

Increasing δ also reveals some interesting interplay between the parameterization that allows for the oscillations and the tipping. As increasing δ decreases the ice-stream velocity, the ice sheet loses less mass dynamically and thus the forcing magnitude required for tipping increases. However, the tipping is now no longer delayed by the oscillations. Since the lifetime of the transients can be ~~upwards of~~ over 100 ka, it may be the case that the tipping occurs later for a lower forcing value. Thus the oscillations simultaneously serve to lower the value of the ~~tipping~~ bifurcation point as well as to increase the time before tipping occurs.

4.5 Limitations of the modelling approach

A caveat of the results of this paper is that they are built upon numerical considerations that may be highly sensitive to modelling choices. The coarse resolution of the ice-sheet model results in many small-scale processes, such as those of smaller ice streams or the topographic roughness of outlet stream such as the Petermann fjord, which may introduce additional oceanic forcing that can influence the retreat of the ice extent (Cuzzone et al., 2019). This is particularly important for the PIS, which extends though a fjord and thus its retreat is sensitive to model resolution. However, retreated HIS and PIS observed in the model

does not extend to the ocean, meaning that the chaotic variability observed is due to the ice dynamics and basal hydrology rather than due to connectivity to the ocean and the numerical instabilities associated therewith. Additionally, the retreated HIS and PIS lie on a bed topography that has much lower relief than that of the fjords at the extent of the unretreated PIS (Morlighem et al., 2017), indicating it may not be as sensitive to model resolution (Cuzzone et al., 2019). That being said, vital processes such as calving in fjords cannot be properly represented on coarser resolutions, so whether the PIS would retreat in a way that allows for sustained oscillations is questionable. More directly, it has been demonstrated that the mechanism of the ice stream oscillation itself is resolution-dependent (Hank et al., 2023; Hank and Tarasov, 2024).

The geothermal heat flux is a boundary condition that is highly uncertain but has a critical effect on the behaviour of these surges, as it sets the pace of basal melting and meltwater production that is critical to the transition of an ice stream from the build-up to the surge mode (Hank and Tarasov, 2024). For example, Martos et al. (2018) report much larger geothermal heat fluxes in the region containing the PIS and HIS, which would tend the ice streams towards a steady-streaming mode, leading to a more predictable collapse of the GrIS by avoiding the chaotic transients entirely.

Uncertainties in precipitation fields are yet another limitation, as accumulation rates are vital to maintaining the build-up/surge pattern. If accumulation is too large, the thinning of ice stream due to the surge might not decrease the ice thickness enough to cause re-freezing at the base, maintaining a steady-streaming mode (Robel et al., 2013). A poor estimation of the precipitation rates in the north-western region of Greenland may result in the build-up surge variability never being realized.

Lack of coupling to an oceanic model decreases the impact of marine-terminating glaciers on the collapse of the ice sheet, which are an important but poorly constrained source of ice sheet mass loss (Catania et al., 2020). While there is an oceanic forcing applied in the ramping experiments, it is spatially constant, which may underestimate the warming in the southeast and overestimate it in the northwest (Cowton et al., 2018). A proper implementation of oceanic forcing could induce an ice-sheet collapse that begins in the south, invalidating the presence of the oscillations that delay the tipping. This mechanism may also re-introduce the possibility of r-tipping of the GrIS. There is also no bi-directional coupling between the ice sheet and the ocean, which may serve as a negative feedback (Pöppelmeier and Stocker, 2025; Wunderling et al., 2024) that can prevent the oscillations. This could results in dynamic mass loss of the GrIS that outpaces the period of the oscillations, rendering their effect on the time before tipping invalid.

Another important clarification is that the chaotic transients observed only appear for a very small range of forcing magnitudes past the bifurcation point. This is due to the strong power-law scaling of the chaotic transient lifetime (equation 9), meaning that many other modelling studies that investigate the tipping of the GrIS may only consider temperature forcing values outside of this narrow band. Ultimately, this means the period, amplitude, or even appearance of these surges that generate the chaotic variability are highly dependent on the model configuration and sensitive to parameterization. That is, any misrepresentation of the dynamics due to the numerical modelling considerations might change how often and at what thresholds these surges occur. However, their appearance alone is worthy of investigation and is the purpose of the present study.

5 Conclusions and future work

Setting out to identify whether the GrIS is susceptible to r-tipping, we performed warming experiments at different rates using a comprehensive ice-sheet model. In the course of this line of investigation, it was discovered that the coupled model exhibits a mode of variability that has heretofore not been observed in models of the GrIS. This is presumably because, at least for our model, they only exist for a very small range of external temperature forcing between +1.05 and +1.30 K.

This variability appears in the form of oscillations of ice streams in the ~~present-day~~ GrIS due to thermomechanical coupling at the base of the ice. Warming of the ice sheet causes an initial retreat of the ice extent in the northwest region, resulting in the Petermann and Humboldt glaciers entering a configuration where they experience build-up/surge variability. Due to their proximity, they influence each other and the resulting pattern is chaotic. Since the tipping of the ice sheet begins in the region where these ice streams are found, their presence delays the tipping of the ice sheet to an ice-free state.

The conclusions are limited by the amounts and types of simulations conducted. An obvious next step is to repeat experiments using a different grid size to observe the dependence ~~, if any,~~ of these oscillations on the model domain. ~~A~~ Additionally, sensitivity experiments should be performed to test the dependence of the appearance of these oscillations on the other modelling choices outlined in section 4.5. Further, a full investigation of the phase space and the basins of attraction in the parameter range around the tipping would give a much clearer picture on when the tipping may occur, or if there are multiple closer steady states before a larger tipping. ~~Additionally, an edge-tracking algorithm (Lucarini and Bódai, 2017; Mehling et al., 2024; ?) can be used to approximate the chaotic non-attracting set, even for a ghost attractor. This can be used to identify whether it is such a ghost attractor, or else a chaotic saddle.~~

~~In~~ Most relevantly, a investigation of the nature of these oscillations in the context of the present-day GrIS should be performed, although this requires the detailed sensitivity analyses described above. Then, in connection with other elements of the climate system, the oscillations themselves on a shorter time scale are ~~worth studying~~important to study for their implications on other subsystems of the Earth's climate. For example, ~~they~~ the surges may represent a periodic freshwater forcing condition on the AMOC. If the retreated configuration where oscillations occur is considered as a separate state to the current ice-covered GrIS, r-tipping onto this attractor may be investigated.

The implications of chaotic transients on anthropogenic climate change in this context is phenomenological rather than sociologically relevant, both due to the long time scales of the variability as well as the difference between the initial state of our simulations and the present-day GrIS. Long tipping times might erroneously suggest that the GrIS is stable, although it eventually tips when keeping the forcing parameter constant. On the other hand, ~~these~~ long transients allow for overshooting of the tipping point, whereafter the forcing parameter may still be reduced in time to prevent the tipping.

Code availability

The source code for Yelmo and REMBO can be found at https://github.com/palma-ice/yelmo and https://github.com/alex-robinson/rembo1, respectively.

Author contribution

KK: Conceptualization, Investigation, Visualization, Writing (original draft). **MM:** Conceptualization, Methodology, Software, Writing (review and editing) **AR:** Conceptualization, Methodology, Software, Writing (review and editing) **JA-S:** Conceptualization, Methodology, Software, Writing (review and editing) **JS-J:** Conceptualization, Methodology, Software, Writing (review and editing) **PD:** Conceptualization, Writing (review and editing)

Competing interests

The authors declare that they have no known competing financial interests or personal relationships that could have appeared to influence the work reported in this paper.

Acknowledgments

KK would like to thank Reyk Börner, Oliver Mehling, and Johannes Lohmann for valuable discussions.

Financial support

This project has received funding from the European Union's Horizon 2020 research and innovation programme under the Marie Skłodowska-Curie Innovative Training Network CriticalEarth, grant agreement no. 956170. This is a contribution to the European Union's Horizon 2020 research and innovation programme ClimTip, grant agreement no. 101137601. Alexander Robinson received funding from the European Research Council (ERC Consolidator grant, FORCLIMA, grant no. 101044247). Marisa Montoya received funding from CREEP..

Appendix A: Initial states

Appendix B: Comparison to ice streams in other areas of the GrIS

The variability of the retreated PIS and HIS is unique when comparing them to other ice streams in the model domain. Figure B1 displays the same information as Fig. 9, but with ice streams on the west coast of Greenland in the left-hand-side panels. These glaciers correspond to the Ilulissat/Jakobshavn/Sermeq Kujalleq (blue), Sermeq Avannarleq (green), and Store (red) glaciers. These glaciers are all in the steady-streaming state, indicated by maximal basal water thickness and a constant, nonzero basal velocity. Very slight variations in the mean ice thickness can be seen, but none so great as for the retreated HIS and PIS glaciers that display build-up/surge variability. Notably, these are marine-terminating glaciers, meaning they experience oceanic forcing that promotes basal melting and therefore steady-streaming.

Further comparisons can be made to outlet glaciers in the nearby hydrological basin. Figure B2 indicates the variability in the marine-terminating Upernavik (red and green), Illullip Sermia (blue), and King Oscar (purple) glaciers. Most notably, the

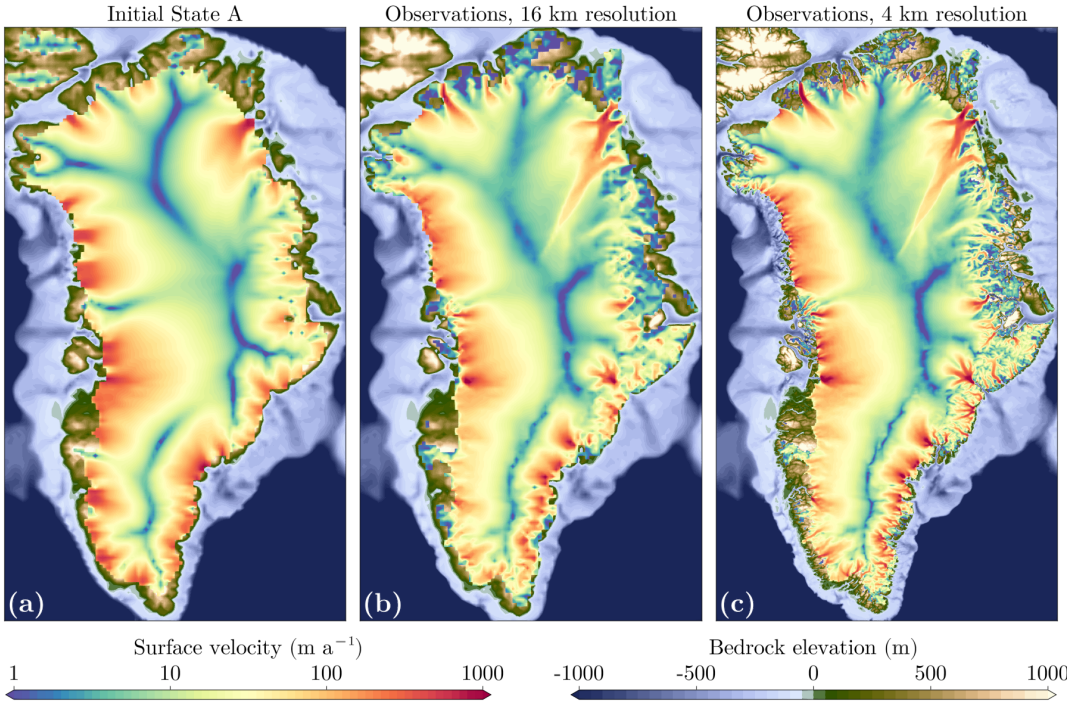

Figure A1. Ice sheet extent and surface velocities for a) initial condition A used in this study; b) surface velocity data of Joughin et al. (2018) at 16 km resolution; c) surface velocity data of Joughin et al. (2018) at 4 km resolution. Panel a is the same as panel b of Fig. 1

King Oscar glacier displays rapid fluctuations in ice thickness and basal velocity, which accounts for the dominant mode of variability in this drainage basin. These fluctuations occur on a much faster time scale than those of the retreated HIS and PIS, with a period around 2 ka.

Figure B3 shows the variability of other glaciers in the west of the GrIS which are not marine-terminating. These ice streams also experience small fluctuations in basal velocity and ice thickness, but the basal water layer thickness does not change as much as in the retreated PIS and HIS.

Appendix C: Comparison to oscillations of the LIS

Large-scale oscillations of ice streams were first proposed as the reason for Heinrich events (HEs) during the last glacial period (LGP) (Heinrich, 1988; Broecker et al., 1992; MacAyeal, 1993), but these events might be caused instead by external forcing (Alvarez-Solas et al., 2013; Bassis et al., 2017). While the variability of the oscillations seen in this study seems similar to the build-up/surge variability seen in most simulations of HEs in the Laurentide ice sheet (LIS) of the LGM ~~(Calov et al., 2002; Papa et al., 2006; Roberts et al., 2016; Ziemen et al., 2019; Schannwell et al., 2023)~~(Calov et al., 2002; Hank and Tara , they do not match exactly. Most notably, the Hudson ice stream in those studies displays a more gradual increase in ice volume

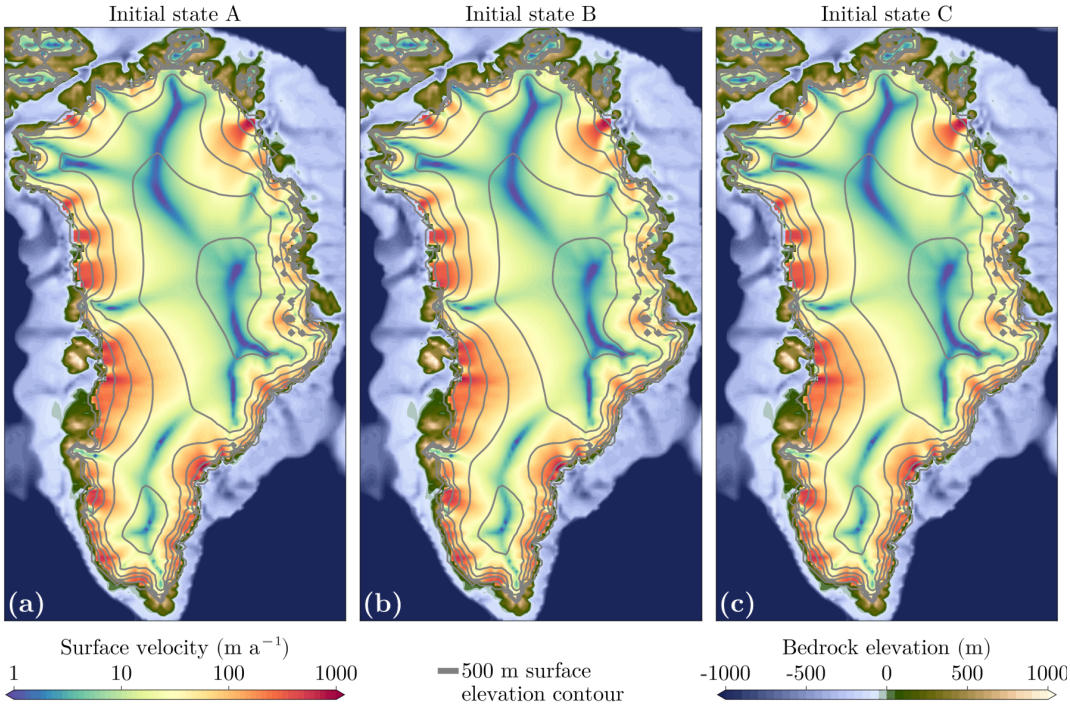

Figure A2. Ice sheet surface velocities for the three different initial states.

followed by a sudden surge. This is in contrast to the pattern in the retreated HIS and retreated PIS in this experiment, where the build-up is either over the same time period (in the case of the short oscillations) or faster (in the case of the longer asymmetric events) than the subsequent surge. Additionally, in the latter case, the ice loss accelerates over time, rather than being maximal at the beginning of the surge. It may be the case that the variability seen in the GrIS, while having the same physical mechanism of thermo-mechanical coupling, may have a source additional of variability, i.e. the spatial interaction of the retreated PIS and retreated HIS, that causes it to behave differently from these experiments of a single oscillating ice stream.

Common to ice-sheet model simulations of the LIS are oscillations in ice-sheet volume that sometimes show quasiperiodicity or seemingly chaotic behaviour. It would be expected that, due to the large spatial extent of the system and the complex basal topography, the oscillations would not have a near-constant period. Even in the idealized geometry of Calov et al. (2010) there is spontaneous spatial asymmetry that leads to inconsistent oscillatory frequency. Such irregular variability is of special importance when studying the tipping behaviour of a system. Still, without an ensemble of simulations starting from similar initial conditions, it is unknown how irregular the variability seen in these studies is.

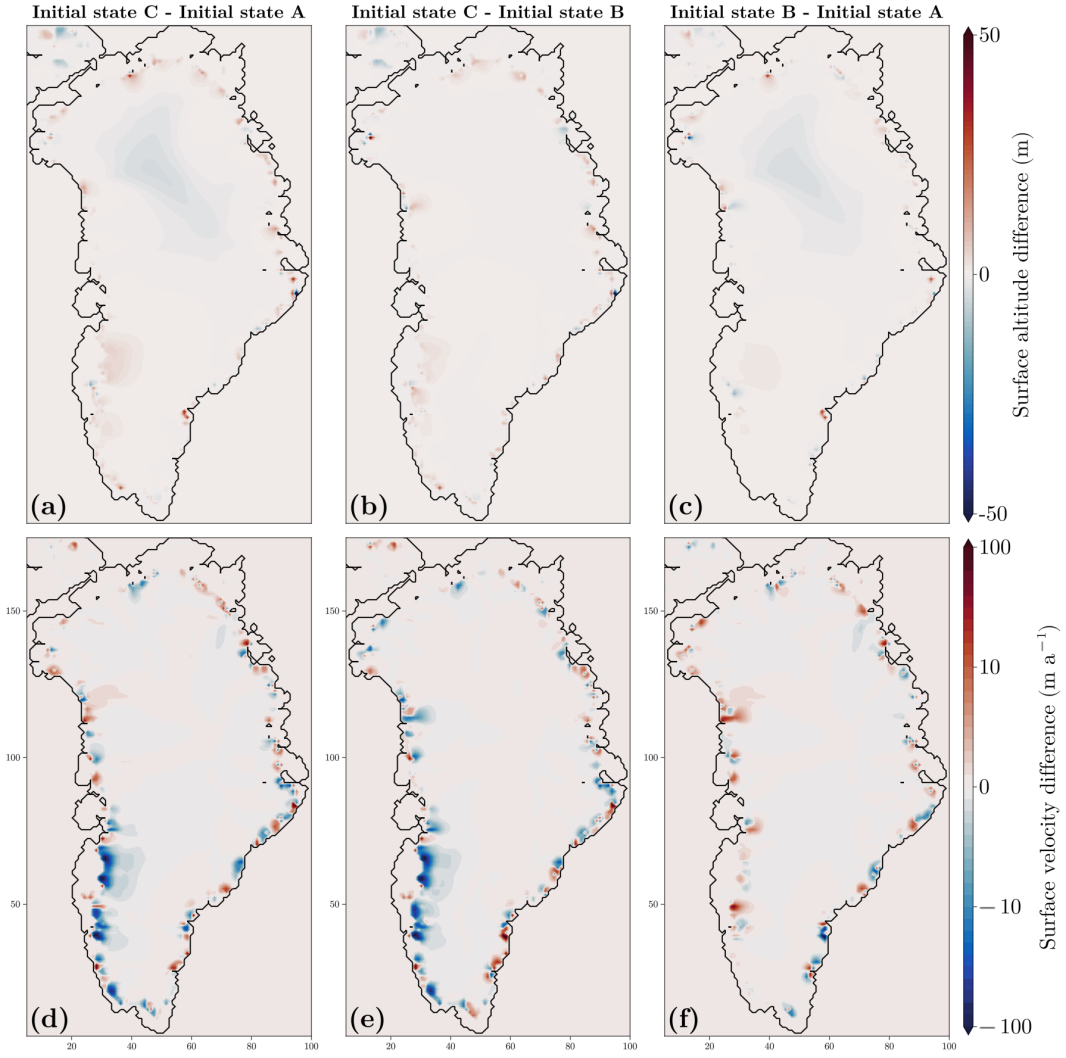

Figure A3. Differences in surface altitude and surface velocity between the three initial states.

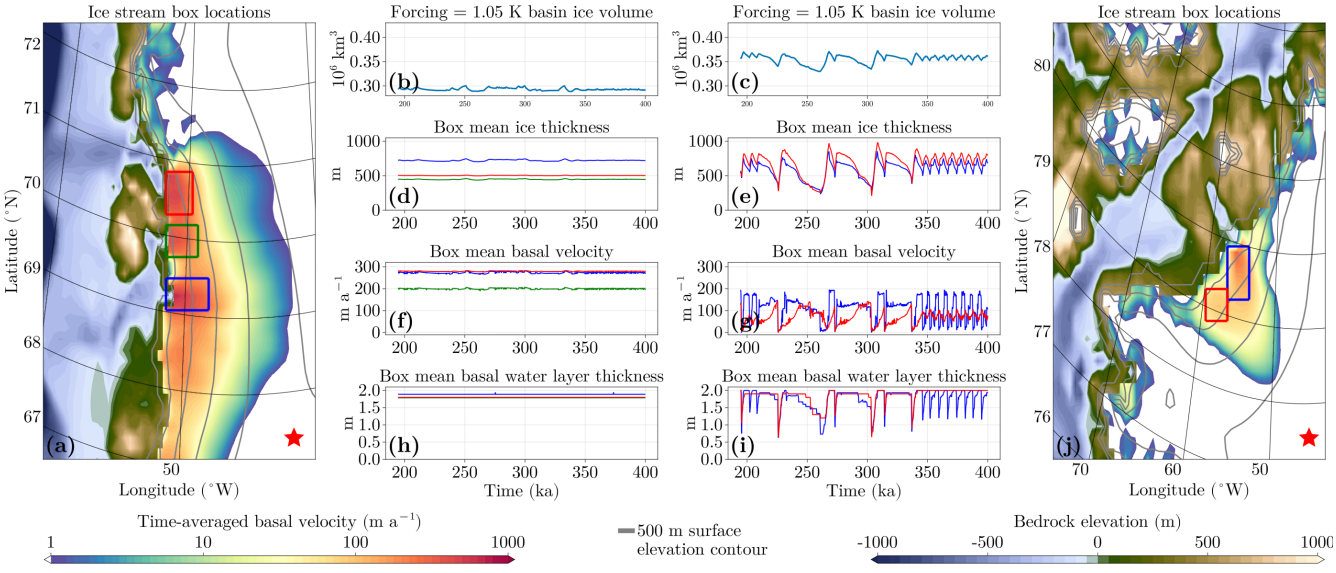

Figure B1. As Fig. 9, but with ice-streams on the west coast of Greenland between 67 and 72 ° N compared to the retreated PIS and HIS

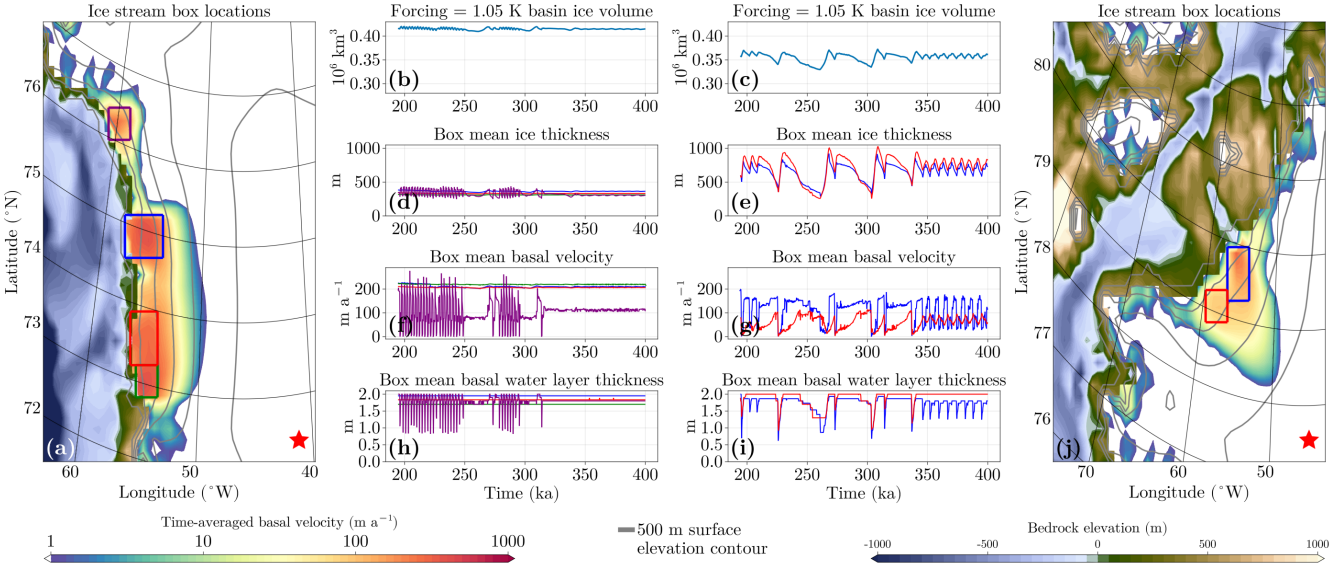

Figure B2. As Fig. 9, but with ice-streams on the west coast of Greenland between 72 and 76 ° N compared to the retreated PIS and HIS

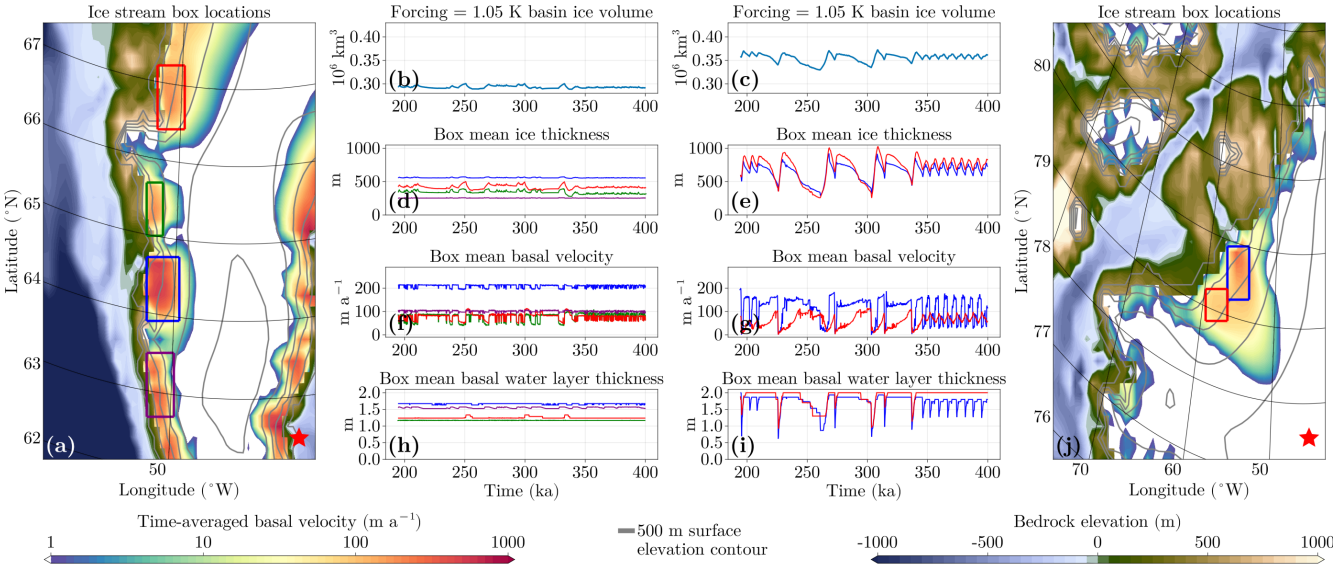

Figure B3. As Fig. 9, but with ice-streams on the west coast of Greenland between 62 and 67 ° N compared to the retreated PIS and HIS

Appendix D: ~~Link to nonlinear dynamics~~Transient lifetime for a forcing value of 1.05 K

D1 ~~Chaotic transients~~

~~Systems that experience chaotic variability have long transients with lifetimes of indeterminate length, and these are hence called chaotic transients (Lai and Tél, 2011). Specifically, the lifetime of any chaotic transient depends sensitively on its initial condition, but the lifetimes of an ensemble are exponentially distributed. These chaotic transients are due to the existence of chaotic non-attracting sets, the most relevant being chaotic 'ghost attractors' and chaotic saddles. The distinction is important, as the ghost attractor exists in the monostable parameter regime, whereas the chaotic saddle exists in the bistable parameter regime.~~

~~A chaotic ghost attractor materializes as a result of a chaotic attractor undergoing a boundary crisisdue to a continuously changing parameter (Grebogi et al., 1982), essentially a chaotic analogue of a saddle-node bifurcation. A trajectory that is forced beyond this crisis parameter value will remain around the ghost attractor for some time before eventually tipping, causing the chaotic transient. On the other hand, a chaotic saddle lies on the basin boundary that separates two co-existing attractors. It generates long-lived transients when a trajectory crosses this basin boundary, as solutions are captured by the attracting manifolds of the saddle before eventually approaching one of the two attractors. Such a phenomenon in the context of r-tipping has been previously reported in a study by Lohmann and Ditlevsen (2021) for the Atlantic Meridional Overturning Circulation (AMOC). In their study, trajectories forced at different rates are brought close to the basin boundary between the stable 'AMOC on' state and the chaotic saddle that separates it from the stable 'AMOC off' state. As the basin boundary is~~

fractal, differing rates may cause it to tip or not in a non-monotonic way. For a chaotic saddle, the mean lifetime of chaotic transients scales with the fractal dimension of the saddle (Hunt et al., 1996; Mehling et al., 2024; Sweet and Ott, 2000).

Due to being a transient simulation, the AQEF itself may exhibit a chaotic transient. The biggest evidence for this is comparing the simulations ramped to Figure 7 sees a marked difference between the mean ice volume at a forcing magnitude of +1.25 K and 1.30 K. If the oscillations are due to crossing a chaotic saddle before the tipping point of 1.275 K is reached (i.e those simulations for 1.00K when compared to those with +1.25 K), then they must be qualitatively different from the ghost attractor generated by a boundary crisis after the boundary crisis (i. e those for +1.30 K), as 1.05 K and greater, suggesting there is an 'edge state' inhabited by the latter. This edge state would be the chaotic saddle only exists in the bistable parameter regime and the ghost attractor only exists in the monostable parameter regime. However, the trajectories at both forcing values occupy the same regions of phase space before tipping, implying that they are the same type of chaotic transient. This implies that the bifurcation that lies between the stable ice-covered GrIS and collapsed GrIS states. To reinforce the argument that r-tipping does not occurbetween +1.25 K and 1.30 K. Similar reasoning can be applied to all parameter values that result in tipping. Thus, the bifurcation point is either between +1.05 K and 1.10 K and all transients are due to a ghost attractor, or the tipping point is larger than +1.30 K and all of the transients are due to an r-tipping through a , it would need to be demonstrated that this is not a chaotic saddle. One method is to apply an edge-tracking algorithm that can approximate this non-attracting set (Lucarini and Bódai, 2017; Mehling et al., 2024; Börner et al., 2025), which is the subject of future work.

The behaviour of the chaotic transients in the present study more closely resembles those due to a boundary crisis than crossing a chaotic saddle. First, scaling laws indicate that the lifetime of the chaotic saddle, and thereby the tipping time, should increase as the maximal forcing approaches the bifurcation point from the left (Mehling et al., 2024). In contrast, the mean lifetime of the chaotic transients scales with the magnitude of the parameter past the crisis value (Grebogi et al., 1986),

$$\langle \tau \rangle \sim (p - p_c)^{-\gamma},$$

which mirrors the pattern seen in the tipping times in Fig. 5. Secondly, if r-tipping was present, we may expect to see tipping not occur below some critical rate.

D1 Transient lifetime for a forcing value of 1.05 K

The stateof the system It can be reasoned that if this were an edge state, the simulations at a forcing level magnitude of +1.05 K is of interest since it is on the boundary between more predictable patterns and the irregular oscillations of the chaotic transients . None of the simulations at this forcing value are also chaotic transients and should eventually tip to an ice free stateafter 400 ka of model time, although they exhibit the same variability as those that do tip. In this parameter range, the system may either be either on a chaotic attractor, or otherwise a chaotic transient with a lifetime much ice-free state, but the lifetime is longer than 400 ka.

Using the mean lifetime of the simulations that tipto an ice-free state, the critical exponent in equation 9 can be estimated. Using a maximum likelihood estimation to fit them to an exponential distribution results in a critical exponent of around

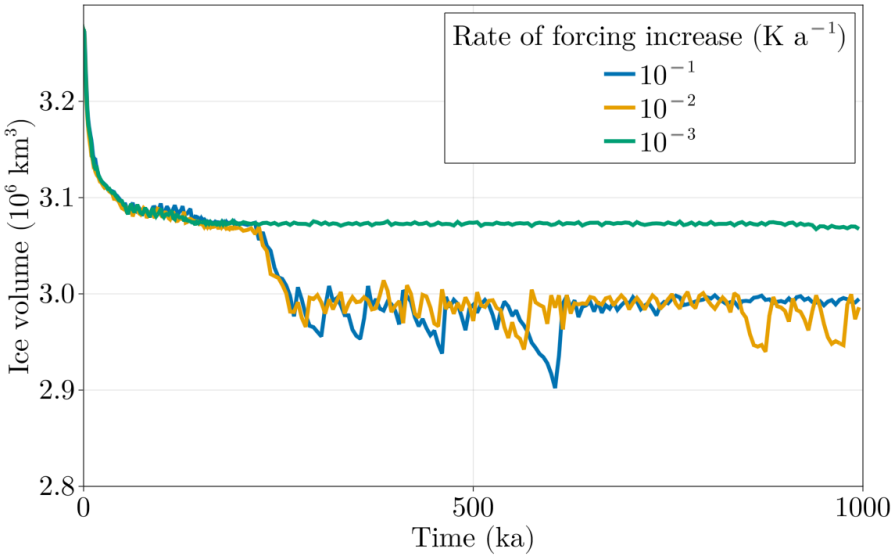

Figure D1. Simulations to 1 Ma for a maximal forcing of +1.05 K at three different rates. This simulation time is estimated to be longer than the mean lifetime of a chaotic transient at this forcing value. The temporal resolution of the output of these simulations for the final 800 ka is 5 ka, in comparison to the 200 a timestep the simulations in Figs. ~~5, 6~~ 7 and ~~8.~~ 9-12

$\gamma \sim 9.959$. Using this, the mean tipping time for a trajectory with a maximal forcing of +1.05 K is around 511 ka, which is indeed longer than the 400 ka simulation run time.

A few additional simulations at this forcing level were done going to 1 Ma and are seen in Fig. ~~10~~D1. None of these simulations tip, suggesting that they are not chaotic transients, but rather motion on a ~~chaotic attractor, and the ice sheet has a~~ genuine chaotic attractor (rather than a ghost) at this parameter value. This further strengthens the argument that the chaotic transients are generated ~~by a boundary crisis, as the resulting~~ ghost attractor due to crossing a bifurcation point, as this ghost attractor is qualitatively similar to the chaotic attractor that exists before the ~~crisis Lai and Tél (2011)~~bifurcation (Lai and Tél, 2011).

D1 ~~Intermediate tipping~~

Appendix E: Intermediate tipping

Within the simulation ensemble, there are a few 'anomalous' runs that do not behave as ~~expected.~~ the others at their forcing magnitudes, as seen in Fig. 14. There are two such types: first, for a forcing level of +1.00 K, one simulation ends up in the retreated configuration with ice-volume variability similar to but slightly smaller in magnitude than those of larger forcing

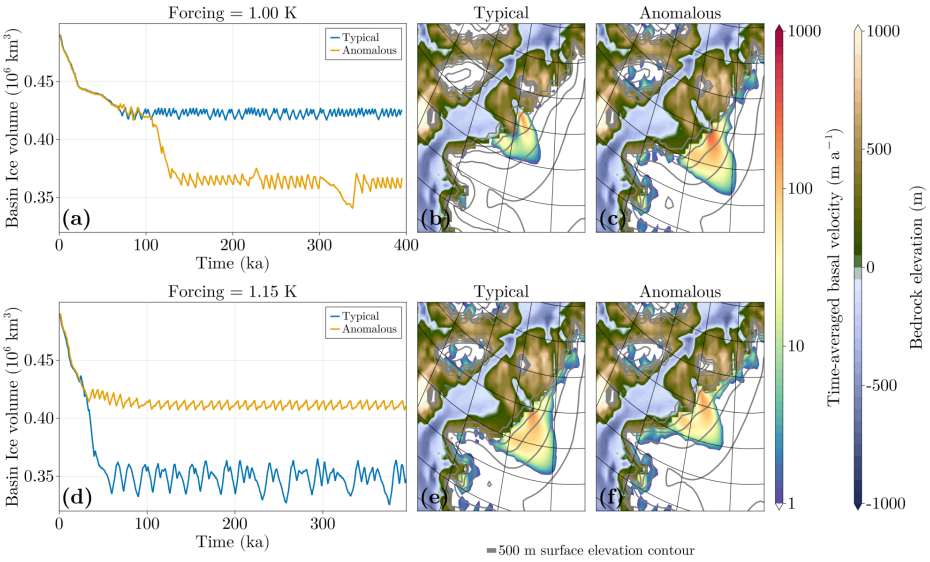

Figure E1. (a): Time series and mean ice thickness for typical and anomalous model trajectories at a forcing of +1.00. (b): Ice sheet extent and time-averaged basal velocity fields of a typical trajectory. (c): Ice sheet extent and time-averaged basal velocity fields of the anomalous trajectory. (d-f): Same as (a-c) but for a forcing of +1.15 K.

values, as seen in Fig. ~~1~~1E1. This might suggest the chaotic attractor associated with the ice-stream oscillations also exists for lower forcing values, albeit with a smaller basin of attraction and thus it has a lower probability of being reached.

Second, there is a simulation with a maximal forcing of +1.15 K that remains in the unretreated configuration. ~~That is, for larger forcing values the less chaotic attractor remains at a diminished size.~~ The 1 Ma simulations for a maximal forcing of +1.05 K in Fig. 10 also show the unretreated configuration is possible at this forcing value. ~~This represents a complication in the analysis, since this parameter value is assumed to be associated the chaotic attractor or its ghost.~~

In this case, the structure of the attractors may be that there is intermediate tipping similar to Lohmann et al. (2024). This would imply that around a forcing value of +1.00 to +1.05 K, there are two attractors for the ice-covered state, corresponding to the retreated and unretreated configurations. The attractor for the retreated GrIS experiences a ~~boundary crisis~~ bifurcation between +1.05 and +1.10 K, with corresponding chaotic transients remaining on the associated ghost attractor. On the other hand, the attractor of the unretreated GrIS experiences a bifurcation at a forcing value slightly larger than +1.15 K. This scenario could then have ~~genuine~~ r-tipping onto either the unretreated or retreated configurations, the latter of which experiences an earlier tipping to an ice-free state, resulting in an indirect r-tipping to the ice-free state. The basin boundary between the two ice-covered attractors could be fractal, leading to nearby initial conditions approaching one or the other (McDonald et al., 1985).

References

Albrecht, T., Winkelmann, R., and Levermann, A.: Glacial-cycle simulations of the Antarctic Ice Sheet with the Parallel Ice Sheet Model (PISM) – Part 2: Parameter ensemble analysis, The Cryosphere, 14, 633–656, https://doi.org/10.5194/tc-14-633-2020, publisher: Copernicus GmbH, 2020.

Alvarez-Solas, J., Robinson, A., Montoya, M., and Ritz, C.: Iceberg discharges of the last glacial period driven by oceanic circulation changes, Proceedings of the National Academy of Sciences, 110, 16 350–16 354, https://doi.org/10.1073/pnas.1306622110, 2013.

An, S.-I., Kim, H.-J., and Kim, S.-K.: Rate-Dependent Hysteresis of the Atlantic Meridional Overturning Circulation System and Its Asymmetric Loop, Geophysical Research Letters, 48, e2020GL090 132, https://doi.org/10.1029/2020GL090132, _eprint: https://onlinelibrary.wiley.com/doi/pdf/10.1029/2020GL090132, 2021.

Armstrong McKay, D. I., Staal, A., Abrams, J. F., Winkelmann, R., Sakschewski, B., Loriani, S., Fetzer, I., Cornell, S. E., Rockström, J., and Lenton, T. M.: Exceeding 1.5°C global warming could trigger multiple climate tipping points, Science (New York, N.Y.), 377, eabn7950, https://doi.org/10.1126/science.abn7950, 2022.

Ashwin, P., Wieczorek, S., Vitolo, R., and Cox, P.: Tipping points in open systems: bifurcation, noise-induced and rate-dependent examples in the climate system, Philosophical Transactions of the Royal Society A: Mathematical, Physical and Engineering Sciences, 370, 1166–1184, https://doi.org/10.1098/rsta.2011.0306, publisher: Royal Society, 2012.

Bassis, J. N., Petersen, S. V., and Mac Cathles, L.: Heinrich events triggered by ocean forcing and modulated by isostatic adjustment, Nature, 542, 332–334, https://doi.org/10.1038/nature21069, publisher: Nature Publishing Group, 2017.

Beem, L. H., Tulaczyk, S. M., King, M. A., Bougamont, M., Fricker, H. A., and Christoffersen, P.: Variable deceleration of Whillans Ice Stream, West Antarctica, Journal of Geophysical Research: Earth Surface, 119, 212–224, https://doi.org/10.1002/2013JF002958, 2014.

Bevis, M., Harig, C., Khan, S. A., Brown, A., Simons, F. J., Willis, M., Fettweis, X., Van Den Broeke, M. R., Madsen, F. B., Kendrick, E., Caccamise, D. J., Van Dam, T., Knudsen, P., and Nylen, T.: Accelerating changes in ice mass within Greenland, and the ice sheet's sensitivity to atmospheric forcing, Proceedings of the National Academy of Sciences, 116, 1934–1939, https://doi.org/10.1073/pnas.1806562116, 2019.

Bintanja, R., Van De Wal, R., and Oerlemans, J.: Global ice volume variations through the last glacial cycle simulated by a 3-D ice-dynamical model, Quaternary International, 95-96, 11–23, https://doi.org/10.1016/S1040-6182(02)00023-X, 2002.

Blasco, J., Tabone, I., Moreno-Parada, D., Robinson, A., Alvarez-Solas, J., Pattyn, F., and Montoya, M.: Antarctic tipping points triggered by the mid-Pliocene warm climate, Climate of the Past, 20, 1919–1938, https://doi.org/10.5194/cp-20-1919-2024, publisher: Copernicus GmbH, 2024.

Bochow, N., Poltronieri, A., Robinson, A., Montoya, M., Rypdal, M., and Boers, N.: Overshooting the critical threshold for the Greenland ice sheet, Nature, 622, 528–536, https://doi.org/10.1038/s41586-023-06503-9, number: 7983 Publisher: Nature Publishing Group, 2023.

Börner, R., Mehling, O., von Hardenberg, J., and Lucarini, V.: Global stability of the Atlantic overturning circulation: Edge state, long transients and boundary crisis under CO2 forcing, Philosophical Transactions of the Royal Society A, https://doi.org/10.1098/rsta.2025.0087, 2025.

Box, J. E., Hubbard, A., Bahr, D. B., Colgan, W. T., Fettweis, X., Mankoff, K. D., Wehrlé, A., Noël, B., Van Den Broeke, M. R., Wouters, B., Bjørk, A. A., and Fausto, R. S.: Greenland ice sheet climate disequilibrium and committed sea-level rise, Nature Climate Change, 12, 808–813, https://doi.org/10.1038/s41558-022-01441-2, 2022.

Broecker, W., Bond, G., Klas, M., Clark, E., and McManus, J.: Origin of the northern Atlantic's Heinrich events, Climate Dynamics, 6, 265–273, https://doi.org/10.1007/BF00193540, 1992.

Brondex, J., Gagliardini, O., Gillet-Chaulet, F., and Durand, G.: Sensitivity of grounding line dynamics to the choice of the friction law, Journal of Glaciology, 63, 854–866, https://doi.org/10.1017/jog.2017.51, 2017.

Brondex, J., Gillet-Chaulet, F., and Gagliardini, O.: Sensitivity of centennial mass loss projections of the Amundsen basin to the friction law, The Cryosphere, 13, 177–195, https://doi.org/10.5194/tc-13-177-2019, 2019.

Budd, W. F.: A First Simple Model for Periodically Self-Surging Glaciers, Journal of Glaciology, 14, 3–21, https://doi.org/10.3189/S0022143000013344, 1975.

Bueler, E. and van Pelt, W.: Mass-conserving subglacial hydrology in the Parallel Ice Sheet Model version 0.6, Geoscientific Model Development, 8, 1613–1635, https://doi.org/10.5194/gmd-8-1613-2015, publisher: Copernicus GmbH, 2015.

Calov, R., Ganopolski, A., Petoukhov, V., Claussen, M., and Greve, R.: Large-scale instabilities of the Laurentide ice sheet simulated in a fully coupled climate-system model, Geophysical Research Letters, 29, https://doi.org/10.1029/2002GL016078, 2002.

Calov, R., Greve, R., Abe-Ouchi, A., Bueler, E., Huybrechts, P., Johnson, J. V., Pattyn, F., Pollard, D., Ritz, C., Saito, F., and Tarasov, L.: Results from the Ice-Sheet Model Intercomparison Project–Heinrich Event Intercomparison (ISMIP HEINO), Journal of Glaciology, 56, 371–383, https://doi.org/10.3189/002214310792447789, 2010.

Carr, J., Vieli, A., Stokes, C., Jamieson, S., Palmer, S., Christoffersen, P., Dowdeswell, J., Nick, F., Blankenship, D., and Young, D.: Basal topographic controls on rapid retreat of Humboldt Glacier, northern Greenland, Journal of Glaciology, 61, 137–150, https://doi.org/10.3189/2015JoG14J128, 2015.

Catania, G., Hulbe, C., Conway, H., Scambos, T., and Raymond, C.: Variability in the mass flux of the Ross ice streams, West Antarctica, over the last millennium, Journal of Glaciology, 58, 741–752, https://doi.org/10.3189/2012JoG11J219, 2012.

Catania, G. A., Scambos, T. A., Conway, H., and Raymond, C. F.: Sequential stagnation of Kamb Ice Stream, West Antarctica, Geophysical Research Letters, 33, 2006GL026 430, https://doi.org/10.1029/2006GL026430, 2006.

Catania, G. A., Stearns, L. A., Moon, T. A., Enderlin, E. M., and Jackson, R. H.: Future Evolution of Greenland's Marine-Terminating Outlet Glaciers, Journal of Geophysical Research: Earth Surface, 125, e2018JF004 873, https://doi.org/10.1029/2018JF004873, _eprint: https://agupubs.onlinelibrary.wiley.com/doi/pdf/10.1029/2018JF004873, 2020.

Choi, Y., Morlighem, M., Rignot, E., and Wood, M.: Ice dynamics will remain a primary driver of Greenland ice sheet mass loss over the next century, Communications Earth & Environment, 2, 26, https://doi.org/10.1038/s43247-021-00092-z, 2021.

Clarke, G. K. C.: Fast glacier flow: Ice streams, surging, and tidewater glaciers, Journal of Geophysical Research: Solid Earth, 92, 8835–8841, https://doi.org/10.1029/JB092iB09p08835, 1987.

Cowton, T. R., Sole, A. J., Nienow, P. W., Slater, D. A., and Christoffersen, P.: Linear response of east Greenland's tidewater glaciers to ocean/atmosphere warming, Proceedings of the National Academy of Sciences, 115, 7907–7912, https://doi.org/10.1073/pnas.1801769115, 2018.

Cuzzone, J. K., Schlegel, N.-J., Morlighem, M., Larour, E., Briner, J. P., Seroussi, H., and Caron, L.: The impact of model resolution on the simulated Holocene retreat of the southwestern Greenland ice sheet using the Ice Sheet System Model (ISSM), The Cryosphere, 13, 879–893, https://doi.org/10.5194/tc-13-879-2019, 2019.

Ehrenfeucht, S., Morlighem, M., Rignot, E., Dow, C. F., and Mouginot, J.: Seasonal Acceleration of Petermann Glacier, Greenland, From Changes in Subglacial Hydrology, Geophysical Research Letters, 50, e2022GL098 009, https://doi.org/10.1029/2022GL098009, _eprint: https://onlinelibrary.wiley.com/doi/pdf/10.1029/2022GL098009, 2023.

Enderlin, E. M., Howat, I. M., Jeong, S., Noh, M.-J., van Angelen, J. H., and van den Broeke, M. R.: An improved mass budget for the Greenland ice sheet, Geophysical Research Letters, 41, 866–872, https://doi.org/10.1002/2013GL059010, _eprint: https://onlinelibrary.wiley.com/doi/pdf/10.1002/2013GL059010, 2014.

Feldmann, J. and Levermann, A.: From cyclic ice streaming to Heinrich-like events: the grow-and-surge instability in the Parallel Ice Sheet Model, The Cryosphere, 11, 1913–1932, https://doi.org/10.5194/tc-11-1913-2017, publisher: Copernicus GmbH, 2017.

Feldmann, J., Klose, A. K., Albrecht, T., and Winkelmann, R.: Rate-induced tipping of ice sheets due to visco-elastic Earth response under idealized conditions, https://doi.org/10.5194/egusphere-2025-5859, 2025.

Feudel, U.: Rate-induced tipping in ecosystems and climate: the role of unstable states, basin boundaries and transient dynamics, Nonlinear Processes in Geophysics, 30, 481–502, https://doi.org/10.5194/npg-30-481-2023, publisher: Copernicus GmbH, 2023.

Fowler, A. C. and Johnson, C.: Ice-sheet surging and ice-stream formation, Annals of Glaciology, 23, 68–73, https://doi.org/10.3189/S0260305500013276, 1996.

Goldberg, D. N.: A variationally derived, depth-integrated approximation to a higher-order glaciological flow model, Journal of Glaciology, 57, 157–170, https://doi.org/10.3189/002214311795306763, publisher: International Glaciological Society, 2011.

Grebogi, C., Ott, E., and Yorke, J. A.: Chaotic Attractors in Crisis, Physical Review Letters, 48, 1507–1510, https://doi.org/10.1103/PhysRevLett.48.1507, publisher: American Physical Society, 1982.

Grebogi, C., Ott, E., and Yorke, J. A.: Critical Exponent of Chaotic Transients in Nonlinear Dynamical Systems, Physical Review Letters, 57, 1284–1287, https://doi.org/10.1103/PhysRevLett.57.1284, publisher: American Physical Society, 1986.

Greene, C. A., Gardner, A. S., Wood, M., and Cuzzone, J. K.: Ubiquitous acceleration in Greenland Ice Sheet calving from 1985 to 2022, Nature, 625, 523–528, https://doi.org/10.1038/s41586-023-06863-2, 2024.

Gregory, J. M., Huybrechts, P., and Raper, S. C. B.: Threatened loss of the Greenland ice-sheet, Nature, 428, 616–616, https://doi.org/10.1038/428616a, publisher: Nature Publishing Group, 2004.

Gutiérrez-González, L., Robinson, A., Alvarez-Solas, J., Tabone, I., Swierczek-Jereczek, J., Moreno-Parada, D., and Montoya, M.: Hysteresis of the Greenland ice sheet from the Last Glacial Maximum to the future, The Cryosphere, 20, 1139–1162, https://doi.org/10.5194/tc-20-1139-2026, 2026.

Hank, K. and Tarasov, L.: The comparative role of physical system processes in Hudson Strait ice stream cycling: a comprehensive model-based test of Heinrich event hypotheses, Climate of the Past, 20, 2499–2524, https://doi.org/10.5194/cp-20-2499-2024, 2024.

Hank, K., Tarasov, L., and Mantelli, E.: Modeling sensitivities of thermally and hydraulically driven ice stream surge cycling, Geoscientific Model Development, 16, 5627–5652, https://doi.org/10.5194/gmd-16-5627-2023, 2023.

Heinrich, H.: Origin and Consequences of Cyclic Ice Rafting in the Northeast Atlantic Ocean During the Past 130,000 Years, Quaternary Research, 29, 142–152, https://doi.org/10.1016/0033-5894(88)90057-9, 1988.

Hillebrand, T. R., Hoffman, M. J., Perego, M., Price, S. F., and Howat, I. M.: The contribution of Humboldt Glacier, northern Greenland, to sea-level rise through 2100 constrained by recent observations of speedup and retreat, The Cryosphere, 16, 4679–4700, https://doi.org/10.5194/tc-16-4679-2022, 2022.

Holland, D. M., Thomas, R. H., de Young, B., Ribergaard, M. H., and Lyberth, B.: Acceleration of Jakobshavn Isbræ triggered by warm subsurface ocean waters, Nature Geoscience, 1, 659–664, https://doi.org/10.1038/ngeo316, publisher: Nature Publishing Group, 2008.

Howat, I. M., Joughin, I., Fahnestock, M., Smith, B. E., and Scambos, T. A.: Synchronous retreat and acceleration of southeast Greenland outlet glaciers 2000–06: ice dynamics and coupling to climate, Journal of Glaciology, 54, 646–660, https://doi.org/10.3189/002214308786570908, 2008.

Hunt, B. R., Ott, E., and Yorke, J. A.: Fractal dimensions of chaotic saddles of dynamical systems, Physical Review E, 54, 4819–4823, https://doi.org/10.1103/PhysRevE.54.4819, 1996.

Höning, D., Willeit, M., Calov, R., Klemann, V., Bagge, M., and Ganopolski, A.: Multistability and Transient Response of the Greenland Ice Sheet to Anthropogenic CO2 Emissions, Geophysical Research Letters, 50, e2022GL101 827, https://doi.org/10.1029/2022GL101827, _eprint: https://agupubs.onlinelibrary.wiley.com/doi/pdf/10.1029/2022GL101827, 2023.

Intergovernmental Panel On Climate Change (IPCC): Climate Change 2021 – The Physical Science Basis: Working Group I Contribution to the Sixth Assessment Report of the Intergovernmental Panel on Climate Change, Cambridge University Press, 1 edn., ISBN 978-1-00-915789-6, https://doi.org/10.1017/9781009157896, 2023.

Joughin, I., Smith, B. E., Howat, I. M., Scambos, T., and Moon, T.: Greenland flow variability from ice-sheet-wide velocity mapping, Journal of Glaciology, 56, 415–430, https://doi.org/10.3189/002214310792447734, 2010.

Joughin, I., Smith, B. E., and Howat, I. M.: A complete map of Greenland ice velocity derived from satellite data collected over 20 years, Journal of Glaciology, 64, 1–11, https://doi.org/10.1017/jog.2017.73, 2018.

Joughin, I., Smith, B. E., and Schoof, C. G.: Regularized Coulomb Friction Laws for Ice Sheet Sliding: Application to Pine Island Glacier, Antarctica, Geophysical Research Letters, 46, 4764–4771, https://doi.org/10.1029/2019GL082526, _eprint: https://onlinelibrary.wiley.com/doi/pdf/10.1029/2019GL082526, 2019.

Kamb, B., Raymond, C. F., Harrison, W. D., Engelhardt, H., Echelmeyer, K. A., Humphrey, N., Brugman, M. M., and Pfeffer, T.: Glacier Surge Mechanism: 1982-1983 Surge of Variegated Glacier, Alaska, Science, New Series, 227, 469–479, http://www.jstor.org/stable/1694144, 1985.

Khan, S. A., Kjær, K. H., Bevis, M., Bamber, J. L., Wahr, J., Kjeldsen, K. K., Bjørk, A. A., Korsgaard, N. J., Stearns, L. A., Van Den Broeke, M. R., Liu, L., Larsen, N. K., and Muresan, I. S.: Sustained mass loss of the northeast Greenland ice sheet triggered by regional warming, Nature Climate Change, 4, 292–299, https://doi.org/10.1038/nclimate2161, 2014.

Khan, S. A., Bamber, J. L., Rignot, E., Helm, V., Aschwanden, A., Holland, D. M., van den Broeke, M., King, M., Noël, B., Truffer, M., Humbert, A., Colgan, W., Vijay, S., and Kuipers Munneke, P.: Greenland Mass Trends From Airborne and Satellite Altimetry During 2011–2020, Journal of Geophysical Research: Earth Surface, 127, e2021JF006 505, https://doi.org/10.1029/2021JF006505, _eprint: https://agupubs.onlinelibrary.wiley.com/doi/pdf/10.1029/2021JF006505, 2022.

Krabill, W., Hanna, E., Huybrechts, P., Abdalati, W., Cappelen, J., Csatho, B., Frederick, E., Manizade, S., Martin, C., Sonntag, J., Swift, R., Thomas, R., and Yungel, J.: Greenland Ice Sheet: Increased coastal thinning, Geophysical Research Letters, 31, https://doi.org/10.1029/2004GL021533, _eprint: https://onlinelibrary.wiley.com/doi/pdf/10.1029/2004GL021533, 2004.

Kypke, K., Ashwin, P., and Ditlevsen, P.: Chaotic variability in a model of coupled ice streams, https://doi.org/10.48550/arXiv.2510.12525, arXiv:2510.12525 [nlin], 2025.

Lai, Y.-C. and Tél, T.: Transient Chaos, vol. 173 of *Applied Mathematical Sciences*, Springer New York, New York, NY, ISBN 978-1-4419-6986-6 978-1-4419-6987-3, https://doi.org/10.1007/978-1-4419-6987-3, 2011.

Larocca, L. J., Twining–Ward, M., Axford, Y., Schweinsberg, A. D., Larsen, S. H., Westergaard–Nielsen, A., Luetzenburg, G., Briner, J. P., Kjeldsen, K. K., and Bjørk, A. A.: Greenland-wide accelerated retreat of peripheral glaciers in the twenty-first century, Nature Climate Change, 13, 1324–1328, https://doi.org/10.1038/s41558-023-01855-6, 2023.

Lohmann, J. and Ditlevsen, P. D.: Risk of tipping the overturning circulation due to increasing rates of ice melt, Proceedings of the National Academy of Sciences, 118, e2017989 118, https://doi.org/10.1073/pnas.2017989118, 2021.

Lohmann, J., Dijkstra, H. A., Jochum, M., Lucarini, V., and Ditlevsen, P. D.: Multistability and intermediate tipping of the Atlantic Ocean circulation, Science Advances, 10, eadi4253, https://doi.org/10.1126/sciadv.adi4253, publisher: American Association for the Advancement of Science, 2024.

Lucarini, V. and Bódai, T.: Edge states in the climate system: exploring global instabilities and critical transitions, Nonlinearity, 30, R32–R66, https://doi.org/10.1088/1361-6544/aa6b11, 2017.

Luthcke, S. B., Zwally, H. J., Abdalati, W., Rowlands, D. D., Ray, R. D., Nerem, R. S., Lemoine, F. G., McCarthy, J. J., and Chinn, D. S.: Recent Greenland Ice Mass Loss by Drainage System from Satellite Gravity Observations, Science, 314, 1286–1289, https://doi.org/10.1126/science.1130776, 2006.

MacAyeal, D. R.: Binge/purge oscillations of the Laurentide Ice Sheet as a cause of the North Atlantic's Heinrich events, Paleoceanography, 8, 775–784, https://doi.org/10.1029/93PA02200, 1993.

Martin, M. A., Winkelmann, R., Haseloff, M., Albrecht, T., Bueler, E., Khroulev, C., and Levermann, A.: The Potsdam Parallel Ice Sheet Model (PISM-PIK) – Part 2: Dynamic equilibrium simulation of the Antarctic ice sheet, The Cryosphere, 5, 727–740, https://doi.org/10.5194/tc-5-727-2011, publisher: Copernicus GmbH, 2011.

Martos, Y. M., Jordan, T. A., Catalán, M., Jordan, T. M., Bamber, J. L., and Vaughan, D. G.: Geothermal Heat Flux Reveals the Iceland Hotspot Track Underneath Greenland, Geophysical Research Letters, 45, 8214–8222, https://doi.org/10.1029/2018GL078289, _eprint: https://agupubs.onlinelibrary.wiley.com/doi/pdf/10.1029/2018GL078289, 2018.

McDonald, S. W., Grebogi, C., Ott, E., and Yorke, J. A.: Fractal basin boundaries, Physica D: Nonlinear Phenomena, 17, 125–153, https://doi.org/10.1016/0167-2789(85)90001-6, 1985.

Mehling, O., Börner, R., and Lucarini, V.: Limits to predictability of the asymptotic state of the Atlantic Meridional Overturning Circulation in a conceptual climate model, Physica D: Nonlinear Phenomena, 459, 134 043, https://doi.org/10.1016/j.physd.2023.134043, 2024.

Meur, E. L. and Huybrechts, P.: A comparison of different ways of dealing with isostasy: examples from modelling the Antarctic ice sheet during the last glacial cycle, Annals of Glaciology, 23, 309–317, https://doi.org/10.3189/S0260305500013586, 1996.

Millan, R., Jager, E., Mouginot, J., Wood, M. H., Larsen, S. H., Mathiot, P., Jourdain, N. C., and Bjørk, A.: Rapid disintegration and weakening of ice shelves in North Greenland, Nature Communications, 14, 6914, https://doi.org/10.1038/s41467-023-42198-2, 2023.

Morlighem, M., Williams, C. N., Rignot, E., An, L., Arndt, J. E., Bamber, J. L., Catania, G., Chauché, N., Dowdeswell, J. A., Dorschel, B., Fenty, I., Hogan, K., Howat, I., Hubbard, A., Jakobsson, M., Jordan, T. M., Kjeldsen, K. K., Millan, R., Mayer, L., Mouginot, J., Noël, B. P. Y., O'Cofaigh, C., Palmer, S., Rysgaard, S., Seroussi, H., Siegert, M. J., Slabon, P., Straneo, F., van den Broeke, M. R., Weinrebe, W., Wood, M., and Zinglersen, K. B.: BedMachine v3: Complete Bed Topography and Ocean Bathymetry Mapping of Greenland From Multibeam Echo Sounding Combined With Mass Conservation, Geophysical Research Letters, 44, 11,051–11,061, https://doi.org/10.1002/2017GL074954, _eprint: https://onlinelibrary.wiley.com/doi/pdf/10.1002/2017GL074954, 2017.

Oerlemans, J.: A numerical study on cyclic behaviour of polar ice sheets, Tellus A, 35A, 81–87, https://doi.org/10.1111/j.1600-0870.1983.tb00187.x, 1983.

Papa, B. D., Mysak, L. A., and Wang, Z.: Intermittent ice sheet discharge events in northeastern North America during the last glacial period, Climate Dynamics, 26, 201–216, https://doi.org/10.1007/s00382-005-0078-4, 2006.

Payne, A. J.: Limit cycles in the basal thermal regime of ice sheets, Journal of Geophysical Research: Solid Earth, 100, 4249–4263, https://doi.org/10.1029/94JB02778, 1995.

Petrini, M., Scherrenberg, M. D. W., Muntjewerf, L., Vizcaino, M., Sellevold, R., Leguy, G. R., Lipscomb, W. H., and Goelzer, H.: A topographically controlled tipping point for complete Greenland ice sheet melt, The Cryosphere, 19, 63–81, https://doi.org/10.5194/tc-19-63-2025, 2025.

Pöppelmeier, F. and Stocker, T. F.: Mutual stabilization of AMOC and GrIS due to different transient response to warming, Environmental Research Letters, 20, 094 015, https://doi.org/10.1088/1748-9326/adf45a, 2025.

Ridley, J., Gregory, J. M., Huybrechts, P., and Lowe, J.: Thresholds for irreversible decline of the Greenland ice sheet, Climate Dynamics, 35, 1049–1057, https://doi.org/10.1007/s00382-009-0646-0, 2010.

Rignot, E. and Kanagaratnam, P.: Changes in the Velocity Structure of the Greenland Ice Sheet, Science, 311, 986–990, https://doi.org/10.1126/science.1121381, 2006.

Rignot, E., Velicogna, I., van den Broeke, M. R., Monaghan, A., and Lenaerts, J. T. M.: Acceleration of the contribution of the Greenland and Antarctic ice sheets to sea level rise, Geophysical Research Letters, 38, https://doi.org/10.1029/2011GL046583, _eprint: https://onlinelibrary.wiley.com/doi/pdf/10.1029/2011GL046583, 2011.

Rignot, E., Fenty, I., Menemenlis, D., and Xu, Y.: Spreading of warm ocean waters around Greenland as a possible cause for glacier acceleration, Annals of Glaciology, 53, 257–266, https://doi.org/10.3189/2012AoG60A136, 2012.

Robel, A. A., DeGiuli, E., Schoof, C., and Tziperman, E.: Dynamics of ice stream temporal variability: Modes, scales, and hysteresis, Journal of Geophysical Research: Earth Surface, 118, 925–936, https://doi.org/10.1002/jgrf.20072, 2013.

Roberts, W. H. G., Payne, A. J., and Valdes, P. J.: The role of basal hydrology in the surging of the Laurentide Ice Sheet, Climate of the Past, 12, 1601–1617, https://doi.org/10.5194/cp-12-1601-2016, publisher: Copernicus GmbH, 2016.

Robinson, A., Calov, R., and Ganopolski, A.: An efficient regional energy-moisture balance model for simulation of the Greenland Ice Sheet response to climate change, The Cryosphere, 2010.

Robinson, A., Calov, R., and Ganopolski, A.: Multistability and critical thresholds of the Greenland ice sheet, Nature Climate Change, 2, 429–432, https://doi.org/10.1038/nclimate1449, number: 6 Publisher: Nature Publishing Group, 2012.

Robinson, A., Alvarez-Solas, J., Montoya, M., Goelzer, H., Greve, R., and Ritz, C.: Description and validation of the ice-sheet model Yelmo (version 1.0), Geoscientific Model Development, 13, 2805–2823, https://doi.org/10.5194/gmd-13-2805-2020, 2020.

Robinson, A., Goldberg, D., and Lipscomb, W. H.: A comparison of the stability and performance of depth-integrated ice-dynamics solvers, The Cryosphere, 16, 689–709, https://doi.org/10.5194/tc-16-689-2022, 2022.

Sayag, R. and Tziperman, E.: Interaction and variability of ice streams under a triple-valued sliding law and non-Newtonian rheology, Journal of Geophysical Research: Earth Surface, 116, https://doi.org/10.1029/2010JF001839, _eprint: https://onlinelibrary.wiley.com/doi/pdf/10.1029/2010JF001839, 2011.

Scambos, T., Bell, R., Alley, R., Anandakrishnan, S., Bromwich, D., Brunt, K., Christianson, K., Creyts, T., Das, S., DeConto, R., Dutrieux, P., Fricker, H., Holland, D., MacGregor, J., Medley, B., Nicolas, J., Pollard, D., Siegfried, M., Smith, A., Steig, E., Trusel, L., Vaughan, D., and Yager, P.: How much, how fast?: A science review and outlook for research on the instability of Antarctica's Thwaites Glacier in the 21st century, Global and Planetary Change, 153, 16–34, https://doi.org/10.1016/j.gloplacha.2017.04.008, 2017.

Schannwell, C., Mikolajewicz, U., Ziemen, F., and Kapsch, M.-L.: Sensitivity of Heinrich-type ice-sheet surge characteristics to boundary forcing perturbations, Climate of the Past, 19, 179–198, https://doi.org/10.5194/cp-19-179-2023, publisher: Copernicus GmbH, 2023.

Schoof, C.: The Effect of Cavitation on Glacier Sliding, Proceedings: Mathematical, Physical and Engineering Sciences, 461, 609–627, https://www.jstor.org/stable/30046308, publisher: The Royal Society, 2005.

Schoof, C.: Marine ice-sheet dynamics. Part 1. The case of rapid sliding, Journal of Fluid Mechanics, 573, 27–55, https://doi.org/10.1017/S0022112006003570, 2007.

Slater, D. A. and Straneo, F.: Submarine melting of glaciers in Greenland amplified by atmospheric warming, Nature Geoscience, 15, 794–799, https://doi.org/10.1038/s41561-022-01035-9, 2022.

Souček, O. and Martinec, Z.: ISMIP-HEINO experiment revisited: effect of higher-order approximation and sensitivity study, Journal of Glaciology, 57, 1158–1170, https://doi.org/10.3189/002214311798843278, 2011.

Strogatz, S. H.: Nonlinear dynamics and chaos: with applications to physics, biology, chemistry, and engineering, Studies in nonlinearity, Westview Press, Cambridge (Mass.), ISBN 978-0-7382-0453-6, 1994.

Sun, S., Pattyn, F., Simon, E. G., Albrecht, T., Cornford, S., Calov, R., Dumas, C., Gillet-Chaulet, F., Goelzer, H., Golledge, N. R., Greve, R., Hoffman, M. J., Humbert, A., Kazmierczak, E., Kleiner, T., Leguy, G. R., Lipscomb, W. H., Martin, D., Morlighem, M., Nowicki, S., Pollard, D., Price, S., Quiquet, A., Seroussi, H., Schlemm, T., Sutter, J., Van De Wal, R. S. W., Winkelmann, R., and Zhang, T.: Antarctic ice sheet response to sudden and sustained ice-shelf collapse (ABUMIP), Journal of Glaciology, 66, 891–904, https://doi.org/10.1017/jog.2020.67, 2020.

Sweet, D. and Ott, E.: Fractal Dimension of Higher-Dimensional Chaotic Repellors, Physica D: Nonlinear Phenomena, 139, 1–27, https://doi.org/10.1016/S0167-2789(99)00222-5, arXiv:nlin/0003014, 2000.

Swierczek-Jereczek, J., Blasco, J., Robinson, A., Alvarez-Solas, J., and Montoya, M.: Rate-induced tipping in marine-based regions of the Antarctic ice sheet, https://doi.org/10.21203/rs.3.rs-6701284/v1, iSSN: 2693-5015, 2025.

The IMBIE Team: Mass balance of the Greenland Ice Sheet from 1992 to 2018, Nature, 579, 233–239, https://doi.org/10.1038/s41586-019-1855-2, 2020.

Trusel, L. D., Das, S. B., Osman, M. B., Evans, M. J., Smith, B. E., Fettweis, X., McConnell, J. R., Noël, B. P. Y., and Van Den Broeke, M. R.: Nonlinear rise in Greenland runoff in response to post-industrial Arctic warming, Nature, 564, 104–108, https://doi.org/10.1038/s41586-018-0752-4, 2018.

Tsai, C.-Y., Forest, C. E., and Pollard, D.: Assessing the contribution of internal climate variability to anthropogenic changes in ice sheet volume, Geophysical Research Letters, 44, 6261–6268, https://doi.org/10.1002/2017GL073443, _eprint: https://onlinelibrary.wiley.com/doi/pdf/10.1002/2017GL073443, 2017.

Uppala, S. M., KÅllberg, P. W., Simmons, A. J., Andrae, U., Bechtold, V. D. C., Fiorino, M., Gibson, J. K., Haseler, J., Hernandez, A., Kelly, G. A., Li, X., Onogi, K., Saarinen, S., Sokka, N., Allan, R. P., Andersson, E., Arpe, K., Balmaseda, M. A., Beljaars, A. C. M., Berg, L. V. D., Bidlot, J., Bormann, N., Caires, S., Chevallier, F., Dethof, A., Dragosavac, M., Fisher, M., Fuentes, M., Hagemann, S., Hólm, E., Hoskins, B. J., Isaksen, L., Janssen, P. A. E. M., Jenne, R., Mcnally, A. P., Mahfouf, J., Morcrette, J., Rayner, N. A., Saunders, R. W., Simon, P., Sterl, A., Trenberth, K. E., Untch, A., Vasiljevic, D., Viterbo, P., and Woollen, J.: The ERA-40 re-analysis, Quarterly Journal of the Royal Meteorological Society, 131, 2961–3012, https://doi.org/10.1256/qj.04.176, 2005.

van den Akker, T., Lipscomb, W. H., Leguy, G. R., van de Berg, W. J., and van de Wal, R. S. W.: Competing processes determine the long-term impact of basal friction parameterizations for Antarctic mass loss, The Cryosphere, 20, 1217–1235, https://doi.org/10.5194/tc-20-1217-2026, 2026.

Van Den Broeke, M., Bamber, J., Ettema, J., Rignot, E., Schrama, E., Van De Berg, W. J., Van Meijgaard, E., Velicogna, I., and Wouters, B.: Partitioning Recent Greenland Mass Loss, Science, 326, 984–986, https://doi.org/10.1126/science.1178176, 2009.

Van Pelt, W. J. and Oerlemans, J.: Numerical simulations of cyclic behaviour in the Parallel Ice Sheet Model (PISM), Journal of Glaciology, 58, 347–360, https://doi.org/10.3189/2012JoG11J217, 2012.

Verjans, V., Robel, A. A., Ultee, L., Seroussi, H., Thompson, A. F., Ackerman, L., Choi, Y., and Krebs-Kanzow, U.: The Greenland Ice Sheet Large Ensemble (GrISLENS): Simulating the future of Greenland under climate variability, EGUsphere, pp. 1–47, https://doi.org/10.5194/egusphere-2024-4067, publisher: Copernicus GmbH, 2025.

Wake, L. M., Lecavalier, B. S., and Bevis, M.: Glacial Isostatic Adjustment (GIA) in Greenland: a Review, Current Climate Change Reports, 2, 101–111, https://doi.org/10.1007/s40641-016-0040-z, 2016.

Weertman, J.: Stability of the Junction of an Ice Sheet and an Ice Shelf, Journal of Glaciology, 13, 3–11, https://doi.org/10.3189/S0022143000023327, 1974.

Wood, M., Rignot, E., Fenty, I., An, L., Bjørk, A., van den Broeke, M., Cai, C., Kane, E., Menemenlis, D., Millan, R., Morlighem, M., Mouginot, J., Noël, B., Scheuchl, B., Velicogna, I., Willis, J. K., and Zhang, H.: Ocean forcing drives glacier retreat in Greenland, Science Advances, 7, eaba7282, https://doi.org/10.1126/sciadv.aba7282, 2021.

Wunderling, N., Donges, J. F., Kurths, J., and Winkelmann, R.: Interacting tipping elements increase risk of climate domino effects under global warming, Earth System Dynamics, 12, 601–619, https://doi.org/10.5194/esd-12-601-2021, 2021.

Wunderling, N., von der Heydt, A. S., Aksenov, Y., Barker, S., Bastiaansen, R., Brovkin, V., Brunetti, M., Couplet, V., Kleinen, T., Lear, C. H., Lohmann, J., Roman-Cuesta, R. M., Sinet, S., Swingedouw, D., Winkelmann, R., Anand, P., Barichivich, J., Bathiany, S., Baudena, M., Bruun, J. T., Chiessi, C. M., Coxall, H. K., Docquier, D., Donges, J. F., Falkena, S. K. J., Klose, A. K., Obura, D., Rocha, J., Rynders, S., Steinert, N. J., and Willeit, M.: Climate tipping point interactions and cascades: a review, Earth System Dynamics, 15, 41–74, https://doi.org/10.5194/esd-15-41-2024, 2024.

Zeitz, M., Haacker, J. M., Donges, J. F., Albrecht, T., and Winkelmann, R.: Dynamic regimes of the Greenland Ice Sheet emerging from interacting melt–elevation and glacial isostatic adjustment feedbacks, Earth System Dynamics, 13, 1077–1096, https://doi.org/10.5194/esd-13-1077-2022, publisher: Copernicus GmbH, 2022.

Ziemen, F. A., Kapsch, M.-L., Klockmann, M., and Mikolajewicz, U.: Heinrich events show two-stage climate response in transient glacial simulations, Climate of the Past, 15, 153–168, https://doi.org/10.5194/cp-15-153-2019, publisher: Copernicus GmbH, 2019.

Zoet, L. K. and Iverson, N. R.: A slip law for glaciers on deformable beds, Science, 368, 76–78, https://doi.org/10.1126/science.aaz1183, publisher: American Association for the Advancement of Science (AAAS), 2020.